DEVELOPMENT AND OPTIMIZATION OF A POSITRON ANNIHILATION LIFETIME SPECTROMETER TO MEASURE NANOSCALE DEFECTS IN SOLIDS AND BORANE CAGE MOLECULES IN AQUEOUS NITRATE SOLUTIONS

THESIS

Matthew A. Ross, Major, USA

AFIT/GNE/ENP/08-M05

**DEPARTMENT OF THE AIR FORCE
AIR UNIVERSITY**

AIR FORCE INSTITUTE OF TECHNOLOGY

Wright-Patterson Air Force Base, Ohio

AFIT/GNE/ENP/08-M05

DEVELOPMENT AND OPTIMIZATION OF A POSITRON ANNIHILATION
LIFETIME SPECTROMETER TO MEASURE NANOSCALE DEFECTS IN SOLIDS
AND BORANE CAGE MOLECULES IN AQUEOUS NITRATE SOLUTIONS

THESIS

Presented to the Faculty

Department of Engineering Physics

Graduate School of Engineering and Management

Air Force Institute of Technology

Air University

Air Education and Training Command

In Partial Fulfillment of the Requirements for the

Degree of Master of Engineering (Nuclear Engineering)

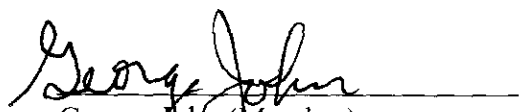Matthew A. Ross, BS

Major, USA

March 2008

DEVELOPMENT AND OPTIMIZATION OF A POSITRON ANNIHILATION
LIFETIME SPECTROMETER TO MEASURE NANOSCALE DEFECTS IN SOLIDS
AND BORANE CAGE MOLECULES IN AQUEOUS NITRATE SOLUTIONS
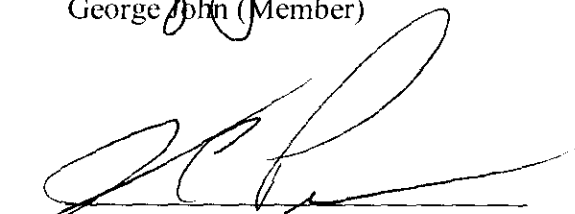
Matthew A. Ross, BS
Major, USA

Approved:

Larry W. Burggraf

Larry Burggraf (Chairman)

17 March 2008

Date

George John

George John (Member)

18 March 2008

Date

James Petrosky (Member)

17 Mar 08

Date

Abstract

A Positron Annihilation Lifetime Spectroscopy (PALS) system was developed and tested. PALS has the capability to characterize negatively charged defects and voids in materials such as explosives. The timing resolution of the optimized system is 197±14 ps as measured with a known ^{60}Co source. A single-crystal tungsten sample was used to confirm the system calibration resulting in a lifetime of 101±2 ps (as compared to 105 ±5 ps in the literature (16)). The PALS system was then used to compare the differences between as grown and neutron-irradiated single crystal silicon carbide (SiC), illustrating that neutron bombardment of SiC results in the creation of silicon vacancies in the material. The lifetime of a positron associated with a boron cage anion, dodecahydrododecaborate in aqueous nitrate solution, was 277 ± 10 ps, compared with previous measurements of the cage compound in solid state which yielded 268 ± 8 ps. Competition for positrons between nitrate anion and the boron cage was measured.

Acknowledgements

I wish to express my gratitude to the faculty and staff of The Air Force Institute of Technology for their guidance and assistance without which this thesis would have presented an insurmountable task.

My fellow classmates have made the process of learning, research and analysis tolerable through their humor and fellow suffering.

"It is a miracle that curiosity survives formal education." - Albert Einstein

"What you've just said is one of the most insanely idiotic things I have ever heard. At no point in your rambling, incoherent response were you even close to anything that could be considered a rational thought. Everyone in this room is now dumber for having listened to it. I award you no points, and may God have mercy on your soul."

– from *Billy Madison*

Table of Contents

List of Figures

List of Tables

DEVELOPMENT AND OPTIMIZATION OF A POSITRON ANNIHILATION

LIFETIME SPECTROMETER TO MEASURE NANOSCALE DEFECTS IN SOLIDS

AND BORANE CAGE MOLECULES IN AQUEOUS NITRATE SOLUTIONS

I. Introduction

The purpose of this thesis is to describe the construction of a fast-fast coincidence timing positron annihilation spectroscopy system (PALS) and its use to measure positron lifetimes in an explosives surrogate material. Actual explosives were not used due to restrictions in place on the laboratory facilities. This work supports research being conducted by the Air Force Research Laboratory on nanoscale pore effects in energetic materials. This thesis assumes the reader has a background understanding of basic nuclear physics.

Background

The objects that surround us, those we see, smell and touch everyday, are composed of matter; molecules made up of atoms which are composed of protons and neutrons in a nucleus surrounded by a cloud of electrons. There is another type of matter with which we are not accustomed: antimatter. For each type of matter there is an equivalent type of antimatter, exactly the same in nearly all ways except for electric charge (there are also anti-neutrons with no charge). When matter and antimatter collide they destroy each other, or annihilate, releasing energy.

Positrons, or positive electrons, were first theorized in 1930 by Paul Dirac (1). He described an electron gas that might have holes in it. These holes would appear as positively charged particles with the same mass as an electron. The positron is predicted by the relativistic wave equation for the energy of the electron, which has two real solutions

$$E = \pm\sqrt{p^2 + mc^2} \qquad (1.1)$$

where the negative solution gives the energy of the electron and the positive solution gives that of the positron. The positron has the same mass as an electron (0.511 MeV or 9.1×10^{-31} kg) and spin (1/2) but opposite charge (1.602×10^{-19} Coulombs). Thus, positrons are the antimatter equivalent to the electron, or the anti-electron. The positron is believed to be a stable particle in a vacuum.

The positron was discovered experimentally by Carl D. Anderson in 1932. His paper, published in 1933, describes his observations of a cloud chamber in which he unexpectedly observed positively charged tracks from cosmic rays (2). By measuring the curvature of the tacks made by charged particles, he determined the particle charge to be equal to that of the proton, but the mass to be on the order of the electron (Figure 1).
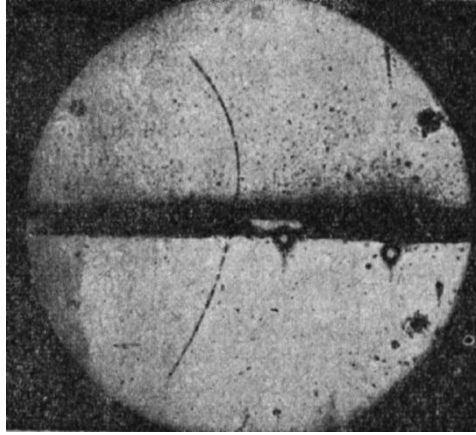
Figure 1. Photograph of a Positron in a Cloud Chamber. [2]

Positrons come from a variety of sources. Reactors and accelerators produce many positrons in their operation. Positrons are also formed through pair-production when the energy of a photon having an energy greater than 1.022 MeV (the rest mass energy of the electron-positron pair) is converted into mass. For laboratory experiments, scientists normally use positrons generated through radioactive decay. Many radioisotopes exist which possess an excess of protons and thus can decay by the $\beta+$ process. $\beta+$ decay occurs when a proton in the nucleus decays into a neutron, emitting a positron accompanied by a neutrino.

$$p \rightarrow n + e^+ + \nu \qquad (1.2)$$

An isotope is chosen as a positron source for a particular application based on a number of considerations. The characteristic half-life of the radioisotope needs to be of sufficient duration such that the activity of the source remains constant, or nearly so, for the duration of the experiment. The half-life must also be adequate for transportation and storage. The activity of the source must be high enough that it is easily identifiable above background, yet not be so high that multiple positrons will be present in the sample at any

one time. The energy of the β+ particle is also of importance; it should stand out from

the background radiation to be easily identifiable in an energy spectrum. In PALS, it is

important to know when the positron is born. This is usually accomplished with a birth

indicator, a gamma emission coincident with the β+ decay. In lifetime spectroscopy the

difference in time between the birth gamma and the annihilation photon is measured,

making the birth gamma extremely important. An important factor in the selection of a

radioisotope is cost. It must be available in sufficient quantities and at a reasonable price.

For these reasons the most commonly used isotope is sodium-22.

Sodium-22, ^{22}Na, has many desirable qualities. ^{22}Na decays by β+ to an excited

state of 22-Neon, ^{22}Ne, 90% of the time. The ^{22}Ne de-excites in 3.7 ps by emitting a

1.274 MeV gamma. The 3.7 ps lifetime is short enough that it can be considered to be

emitted simultaneously with the β+ particle, making it a suitable birth-indicator. ^{22}Na has

a half-life of 2.6 years, long enough to generate a relatively constant β+ flux for the

duration of most experiments. Most importantly, ^{22}Na is readily available and affordable.

The decay scheme is shown in Figure 2.
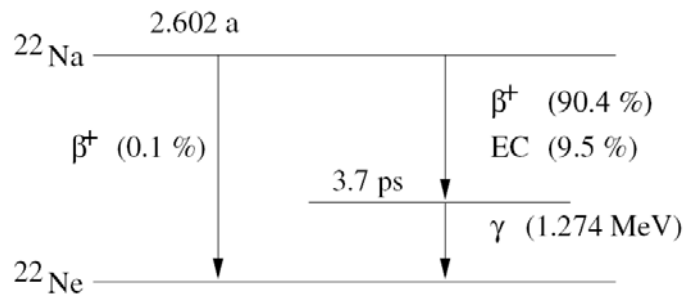
Figure 2. Sodium-22 Decay Scheme.

Positrons are emitted from nuclei in a β+ decay, having a broad spectrum of

energies as shown in Figure 3. The ^{22}Na positron energy spectrum, in particular, has a

peak energy of 546 keV.   For most PALS applications, this range of energies is

acceptable, but for some instances it is desirable to moderate the positrons to a single

energy.
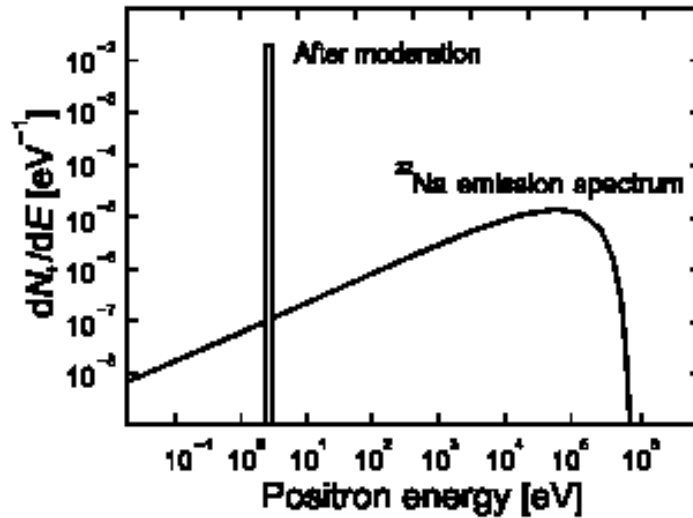
**Figure 3. ^{22}Na positron β+ emission spectrum showing also a
notional moderated positron peak. (18)**

The field of positron spectroscopy consists of three types of techniques. Positron

Annihilation Lifetime Spectroscopy (PALS) measures the time difference between a birth

gamma and an annihilation photon. PALS is a nondestructive method of measuring

defects in materials by relating the lifetime to defect sizes and electron density. Doppler

Broadening of Annihilation Radiation (DBAR) measures the Doppler shift in the photon

energy resulting from the momentum of the annihilating electron-positron pair. It

measures the line width of the annihilation photon energy spectra, detecting changes of a

few percent. DBAR is widely used in the study of defects. The final technique is known

as Angular Correlation of Annihilation Radiation (ACAR) which measures the slight

difference in the angular distribution of the two annihilation photons in the laboratory

frame of reference. In ACAR one detector is stationary while the other is rotated about the sample. The count rate at each angular position is used to obtain an angular correlation curve. For ACAR to obtain good statistics, count times are typically on the order of 100 hours. ACAR gives information on the interactions and annihilation mechanisms of e+.

In a vacuum the positron is a stable particle. However, when it encounters an electron the positron can annihilate. The time it takes from emission, or birth, of a positron to its annihilation can be measured by detecting the gamma rays emitted at the time of each event. The lifetime of a positron in a defect-free media is a property characteristic of the material. However, in a crystalline structure, there are defects such as vacancies or dislocations. The locally reduced electron densities at defect sites result in an increased positron lifetime. The lifetimes of positrons in bulk material are measured and analyzed to determine the relative size and concentration of the defects.

A positron will interact with matter and eventually annihilate with an electron, resulting in the emission of two photons. The lifetime of a positron is determined by measuring the time difference between the gamma photons emitted at its 'birth' in the $\beta+$ decay and those generated at its annihilation. Positron lifetimes are generally on the order of hundreds of picoseconds and vary with the electron density.

Typically, three lifetimes can be obtained from a lifetime spectrum. The first and shortest is associated with positrons interacting with the bulk material, the second with defects in the material and the third with positrons that form a bound state with electrons (positronium).

The benefit of PALS is that it can find smaller defects in lower concentrations than traditional methods such as x-ray diffraction (18). Because of this, PALS is being used in an ever increasing role to measure material defects. Despite the benefits, PALS is not ideal for all applications. For example, it would not be preferable to check for a broken arm by placing someone under a positron beam for 24 hours.

PALS is a common tool at many universities world-wide, and is used by many industries (3). Basic methods used in PALS have not significantly changed since the 1970's, with the exception of the introduction of digitization.

At AFIT, previous work has been done in this field by PhD student Capt Paul Adamson (13). In support of his dissertation, he developed a fast-slow PALS (see Figure 4). He helped set up a similar system for AFRL at Eglin Air Force Base for explosives research.

The fast-slow system uses both anode and dynode outputs from the photomultiplier tube. The anode signal is used to determine timing (fast channel) which is gated by the energy discriminated output from the dynode (slow channel). The benefit of using the fast-slow system is the timing resolution improvement made possible by the energy discrimination. However, this improvement is offset by a much longer counting time.

A fast-fast PALS system uses the anode signal to discriminate the energy of the gamma. A fast-fast setup had not yet been used at AFIT.

A less common PALS technique uses a thin scintillator material to detect the positron itself as opposed to the gamma emitted at the birth of the positron. This method,

called the β+γ coincidence technique, eliminates background and has a high count rate since every positron entering the system is counted (18).
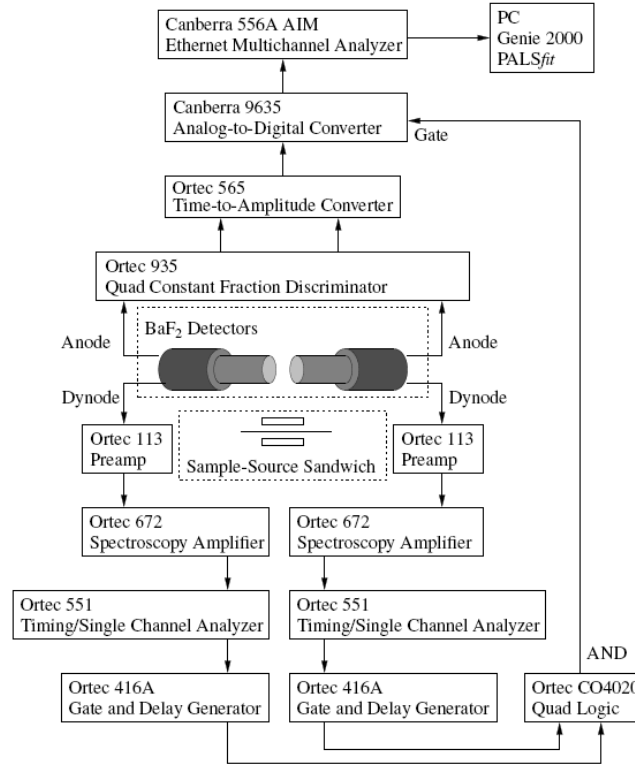
Figure 4. Fast-Slow PALS.

The most recent advancement in PALS technology is digitization. A digital PALS setup takes the pulse from the detector directly into a digitizer. Computer software then analyzes the signal. Digital PALS is becoming used more commonly around the world.

Motivation

This work was sponsored by the Munitions Directorate of AFRL. The U.S. Air Force is becoming interested in using Positron Annihilation Lifetime Spectroscopy (PALS) to qualify and characterize material defects in explosives. Studying these

characteristics can improve production methods and aid in the development of new and improved explosives. This method can also be used to non-destructively test older explosives and support decisions to maintain or replace weapon systems. Captain Paul Adamson and Captain Chris Williams, as part of a collaboration in previous work, set up a PALS system for AFRL/RYMER at Eglin Air Force Base.

It is also important for the military to maintain a technical awareness about the current state of knowledge in the subject of antimatter to monitor for any advancement with possible military application. Future hopes are that a storage mechanism will be discovered to keep many positrons from annihilating for a substantial time. Then large amounts of positrons (10^{15} or more) could be annihilated rapidly, resulting in an anti-matter weapon. One gram of antimatter contains as much energy as a 43 kiloton bomb, without the radioactive debris. Major technological hurdles must be overcome before this much antimatter can be stored. The cage structure of the borane molecule is one possible means of extending the lifetime antimatter.

Scope

This research focuses on developing a PALS system, verifying its accuracy against known values, and applying it to new materials. The materials of interest include as-grown and neutron-irradiated silicon carbide as well as aqueous nitrate/borate solutions. The spectra for each of the materials were analyzed to determine positron lifetimes in the material. The lifetimes provide an indication of material defects in the case of the silicon carbide, and serve as a probe of positron chemistry for the aqueous solutions.

Silicon carbide is of interest to the Department of Defense as a wide band gap semiconductor for many applications. The most critical need is creation of nearly defect free SiC for advanced power in light-weight directed energy microwave weapons.

The intent was to create a reliable system that can be used by future AFIT researchers. This research is a continuation of research performed by Capt Paul Adamson, in which he constructed a PALS system in support of his work on a computational method to estimate positron lifetimes in materials.

Problem Statement

The goal of my research is to construct and optimize a fast-fast PALS system to measure the lifetimes of positrons in crystalline solids and in aqueous nitrate solutions.

To accomplish this I constructed and optimized a fast-fast coincidence timing PALS system. I used this system to collect a timing spectrum on a single crystal tungsten sample for which the annihilation lifetime is well known. This timing spectrum was used to calibrate my results in the PALSfit software by determining the resolution function for the system.

I verified my system by collecting a PALS spectrum on an as-grown SiC wafer and use the calibrated software to determine the positron lifetimes present in the spectrum. The SiC wafer was then neutron-irradiated and a second lifetime spectrum was taken. Pre- and post-irradiation lifetimes were analyzed and compared to determine if any detectable structural changes occurred to the crystal lattice during irradiation.

I also utilized the PALS system to measure the lifetimes of positrons in aqueous solutions to measure the lifetime of positrons associated with the borane cage and with

the nitrate anions. The nitrate anions were observed to inhibit the formation of positronium in the solution by scavenging free electrons. The borane cage competed with the nitrate anions for formation of a longer lived positronium species.

I demonstrated the PALS capability to measure defects in solids and characterize material properties in nitrate matrices relevant to explosives.

II. Theory

This section presents relevant theory of explosives to develop a framework for the importance of this research. It then describes the interactions of positrons with matter. Finally, a discussion on the materials used in the research is presented.

Chemistry of Explosives

Explosives are materials which rapidly produce gas and energy in a chemical reaction. This chemical reaction in most explosives involves molecules consisting of carbon, hydrogen, nitrogen and oxygen. These molecules, when subjected to an activation energy, break down and recombine by oxidation reactions to form more stable molecules at a lower energy, typically CO_2, H_2O and N_2. The energy released by the explosive comes from the energy difference in the molecular bonds between the atoms in the initial and final molecular configurations.

Several properties are used in evaluating explosives, such as density, detonation velocity and detonation pressure. Nanoscale pores in explosive crystalline matrices affect all of these properties. The micro-scale voids create inhomogeneities that allow the formation of hot spots in the explosive. These hot spots form by several methods including: friction between crystals, internal shear within a single crystal and void collapse (4). Hot spots increase the explosive's sensitivity to shock detonation by increasing local temperature and pressure. They also increase the detonation velocity by offering a lower impedance path for the detonation wave. Voids can be introduced intentionally to control the sensitivity of explosives. For insensitive munitions, voids

should be avoided as much as possible. The study of these nanoscale pores can lead to a greater understanding of explosive's behavior. PALS provides a method of studying these nanoscale pores. In this work we use borane cage molecules to simulate nanopores in a matrix.

Another property that affects the performance of explosives is the amount of oxygen available to support the chemical reaction. The initial explosive molecule is originally of the general form $C_xH_yN_wO_z$. The lowest energy oxidized form for carbon is CO_2, for hydrogen it is H_2O, and for nitrogen it is N_2, therefore, an ideal oxidation reaction would result in

$$C_xH_yN_wO_z \rightarrow xCO_2 + \frac{y}{2}H_2O + \frac{w}{2}N_2$$
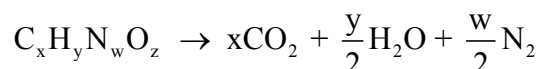
which requires $z \geq 2x + y/2$ for 100% efficiency. However, the explosion is never 100% efficient, resulting in partially oxidized molecules such as CO, H_2 and NO.

Oxygen balance (OB) is a comparison between the total amount of oxygen required to completely oxidize the explosive molecule and the amount of molecular oxygen actually present. This is a relatively simple figure to calculate:

$$OB\% = 100 \; \frac{AW(O)}{MW(\text{explosive})}(z - 2x - y/2) \qquad (1.3)$$

Excess oxygen results in a positive value, while an oxygen deficit results in a negative value. An explosive with an oxygen deficit can produce carbon, resulting in a black cloud after detonation. TNT is an example of an explosive with a low (negative) oxygen balance.

Nitrogen and oxygen are often present in the explosive molecule in the form of nitrates. Nitro groups and nitrates are oxidizing groups; therefore, they are free-electron

scavengers.   In an aqueous solution containing nitrates and positron emitting sodium-22, the nitrate serves to inhibit the formation of positronium (Ps), the bound state of a positron and electron, by scavenging electrons. A portion of this research was concerned with observing the Ps inhibition by nitrate.

TNT is a common explosive widely used as a standard for measuring energy output of other explosives. Its structure is shown in Figure 5. TNT has a molar mass of 227.131 g/mol and a density of 1.654 g/cm^3. It has a chemical composition of: $C_7H_5N_3O_6$. The nitrate ion has a molar mass of 62.0049 g/mol. Since there are two nitrate ions in TNT, the molar fraction of nitrate in TNT is 0.5459. The oxygen balance of TNT is -74%, from equation (1.3):

$$OB\% = 100 \times \frac{16}{227.131} \times \left[6 - (2 \times 7) - \frac{5}{2} \right] = -74\%$$
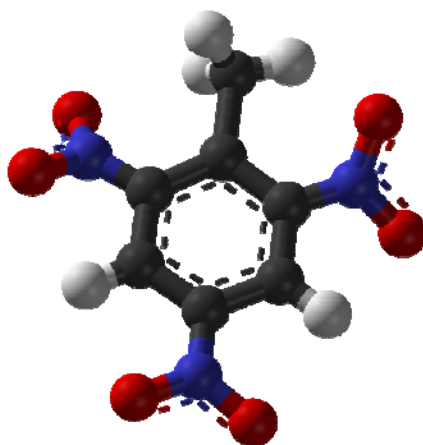
Figure 5. Trinitrotoluene (TNT). Carbon = black; nitrogen = blue; oxygen = red; hydrogen = white.

Nitroglycerin is another common explosive used in dynamite. The chemical formula for nitroglycerine is $C_3H_5(NO_3)_3$ and it has a molar mass of 227.0872 g/mol, and a density of 1.6 g/cm^3 at 15°C. Its oxygen balance is 3.5%. In this molecule it is easier to see the nitrate ions attached to the molecule because nitro groups are bonded to oxygen atoms (Figure 6).
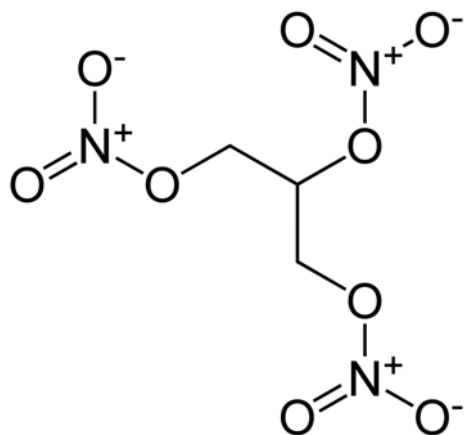
Figure 6. Nitroglycerin

Boranes mixed with nitrate salts are a less common explosive sometimes used for their stability over long periods of time and their insensitivity to shock. Boranes, such as dodecaborane salts mixed with nitrate salts, occasionally are used as propellant in vehicle air bags. The lowest energy form of oxidized boranes is B_2O_3. In this work the dodecaborane cage is used a stimulant for nanoscale voids of constant size.

In the icosahedral borane molecule, $B_{12}H_{12}$, each boron atom at the twelve vertices of an icosahedron is in six-fold coordination, with covalent bonds to an "external" hydrogen atom and five other "internal" boron atoms. This unusual bonding behavior for a group IIA element with a valence of three results in a charge accumulation

about the center of the icosahedron's 20 triangular faces rather than along the lines that link adjacent boron atoms.
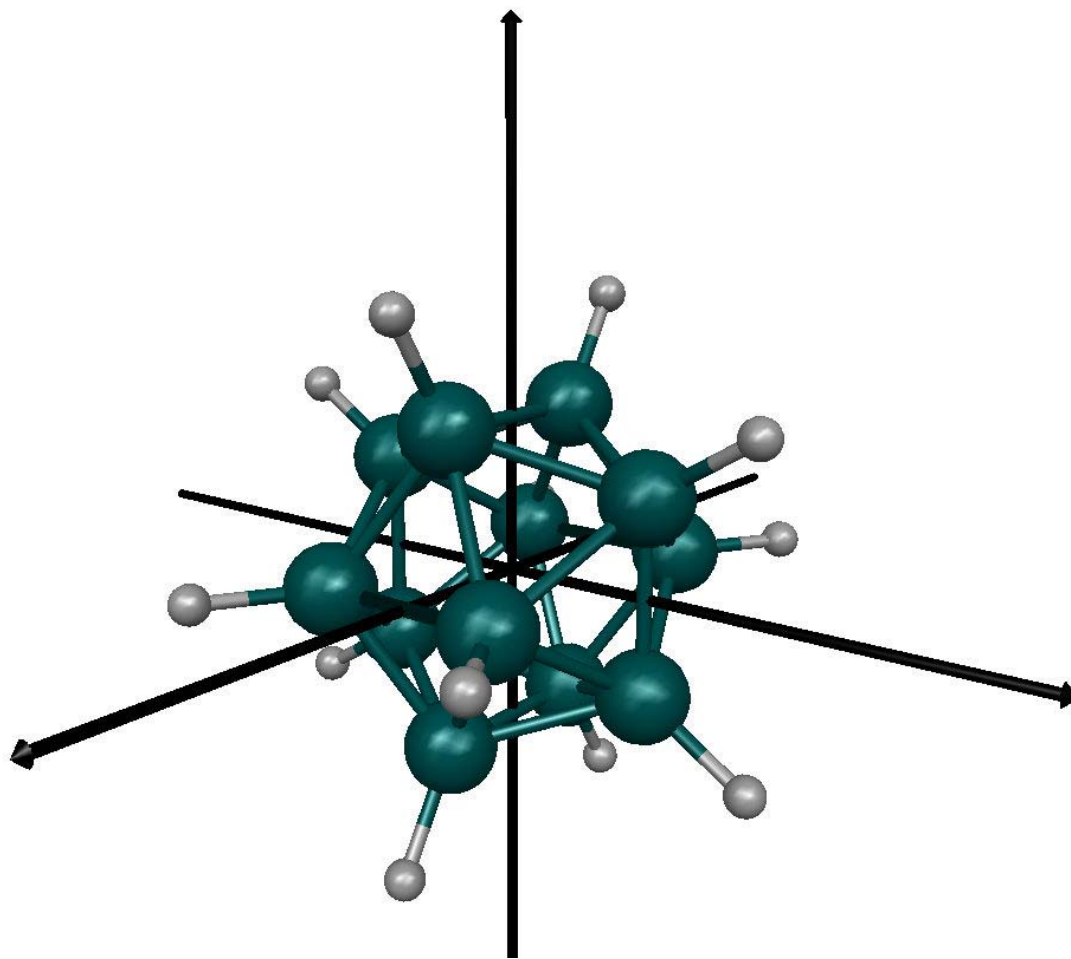
Figure 7. $B_{12}H_{12}$ geometry.

Boron icosahedra readily form dianions and are the main constituents of a large host of insulating refractory solids. For example, in $B_{12}P_2$, $B_{12}As_2$, and $B_{12}O_2$, the B_{12} dianions are centered at the eight vertices of a rhombohedron's longest diagonal, the *c*-axis. Strong covalent bonds link six of the boron atoms of each icosahedron to neighboring icosahedra, and the remaining six boron atoms bond to the solid's cations.

Icosahedral boron-rich solids are generally very hard and have high melting

temperatures. These solids also survive extremely well in high radiation environments, and could find a variety of uses in aerospace applications. This resiliency has been attributed to a "self-healing" process in which a boron atom that is displaced from the icosahedron leaves behind an electron, resulting in a Coulomb attraction that facilitates recombination. The small size of the boron cation also aids in the recombination. Also, the relative stability of the icosahedron relative to the distorted anion caused by knock-on displacement also contributes to the "self-healing". The bond length between boron atoms is 1.8 Å giving an internal radius of 1.36 Å (13).

Positron Interactions with Matter

When a high energy positron enters a material it will interact with the molecular structure largely through scattering interactions with electrons. A high energy positron will lose energy by ionization and electronic excitations of molecules. At high energies, the behavior of the positron is very much like that of an electron due to the equal mass. The positron quickly reaches thermal energies, on the order of a few picoseconds. This thermalization time is short with respect to positron lifetimes in matter and is neglected in the lifetime calculation. The thermalized positron will then travel through the material by diffusion.

The positron can either annihilate with a free electron directly, by electron pick-off or it can form a quasi-stable bound state with an electron (positronium):

$$M + e^+ \rightarrow M^+ + Ps \qquad\qquad (1.4)$$

The positron will annihilate with an electron in a time inversely proportional to the local

electron density in the material. Annihilation can occur by several methods resulting in

zero, one, two, three or more gamma rays (See Figure 8).
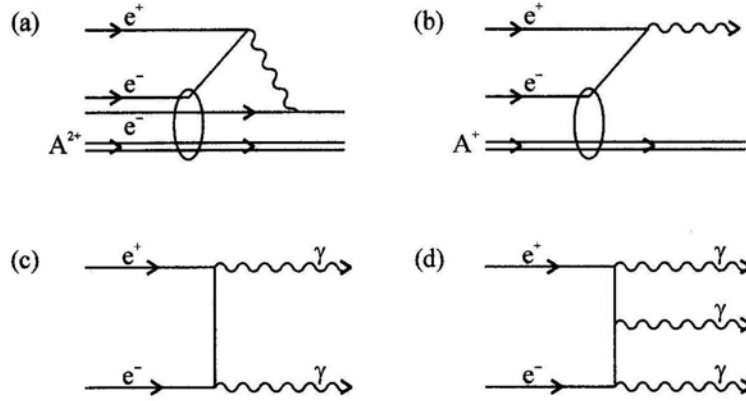
**Figure 8. Feynman diagrams of the lowest order contributions to a) radiationless,
b) one-gamma, c) two-gamma, d) three-gamma ray annihilation. A^{2+} and A^{+} denote
the charge states of the remnant atomic ion. (18)**

For free positrons, the two-gamma annihilation process is the most probable. The

ratio of three to two gamma annihilations is approximately 1/370. Higher numbers of

gamma-emitting annihilation have even lower probability. The zero- and one-gamma

annihilations require a nearby nucleus to conserve energy and momentum, making them

much less probable. For these reasons, positron spectroscopy is generally concerned with

the two-gamma process. The two annihilation gamma rays are emitted collinearly with

respect to the momentum frame of reference. From the laboratory frame, the gammas

differ from linearity slightly, by a few milliradians, due to the angular momentum of the

bound electron-positron pair.

Positronium (Ps) is a bound state of an electron and a positron. Ps is a neutral particle with a binding energy of 6.8 eV. Positronium can exist in one of two spin states. Ortho-positronium is the state in which the spins of the electron and positron are parallel. Para-positronium has anti-parallel spins. The spin configuration greatly affects the lifetime of the positronium atom. Para-positronium annihilates much faster than ortho-positronium (0.125 ns versus 142 ns in vacuum).

The two gamma annihilation rate is much greater than that for the three gamma process (18). Ps forms o-Ps and p-Ps in a 3:1 ratio simply due to spin statistics, but Ps can undergo a spin conversion as it interacts with the surrounding media. The o-Ps can be converted to p-Ps by spin conversion.

Ortho-positronium normally annihilates by a three gamma process in a vacuum. However, in ordinary molecular media the o-Ps can pick-off an electron from the surrounding media that has an anti-parallel spin and then annihilate as para-positronium by the two-gamma process. This pick-off annihilation greatly shortens the lifetime of o-Ps to a few nanoseconds, and causes it to annihilate by two photons rather than three. Even for the longer-lived o-Ps the two gamma annihilation is much more probable than the three gamma annihilation, with the 2γ/3γ ratio being 1115, because ortho-positronium is likely to undergo a spin conversion which causes it to transform into para-positronium (5).

There are two processes for positronium formation. The first, Ore gap theory, proposes that a hot positron picks off an electron as it passes through a medium. The second, recombination theory, says the positron loses its energy through ionization of the medium and then binds to one of the secondary electrons released in the ionization. The

Ore gap model is more suited to describing processes in gases while the recombination process better describes positronium formation in condensed matter. There are two models that describe the recombination process, the spur model and the blob model.

Positrons in Solids

The spur model for positronium formation describes a recombination in which a thermalized positron interacts with an electron from an ionized molecule near the end of the positron's track. In this model, several different reactions are possible, including: ionization, Ps formation, recombination, localization, Ps formation of localized e+, Ps oxidation, and e+ solvation. Solutes that are electron scavengers (such as NO_3^-) inhibit Ps formation, decreasing the intensity of the o-Ps component in the lifetime spectrum by reducing the number of electrons available to interact with the e+.

The blob model is a modification to the spur model, differing in describing the final thermalization and positronium formation in the terminal blob of ionized particles and electrons. The blob model termination consists of about 30 ion-electron pairs, while the spur contains only 2 or 3 (18). The difference is the density of free electrons near the positron.

While there are formulas to determine the size of a void in solids using only the positron lifetime, assumptions have to be made about the geometry of the void and type of interaction. Positrons and Ps can form bound states with anions in the material. These bound states require the use of DBAR or ACAR for size characterization. The bound state lifetimes are too close to those of the free positron lifetime for PALS to resolve the separate lifetime components when more than one species is present.

Positrons in Liquids

The bubble model describes the trapping of Ps in liquids. The Ps atom creates a potential well or bubble in which it gets trapped. In water the radius of this bubble is calculated as 0.291 nm (as compared to .272 nm for borane) resulting in a lifetime of 1.81 ns o-Ps in water (18). Therefore, the lifetime in borane should be slightly shorter than in water. In solids the Ps is trapped in pre-existing defect sites.

Solutes that serve as effective electron scavengers inhibit the formation of positronium by reducing the number of electrons with which positrons can bind. This inhibition reduces the intensity of the Ps lifetime relative to those of the free positrons. It is possible to derive the relationship between lifetime intensity and concentration. The o-Ps intensity (I_3) for different concentrations follows the Stern-Volmer equation

$$I_3(C) = \frac{I_3(0)}{(1+kC)} \qquad (1.5)$$

where C is the concentration of the solute and k is the total inhibition constant. There are two other classes of inhibitors, one that deviates from the Stern-Volmer equation and a second that exhibits a plateau (6).

The PALS system was demonstrated by lifetime measurements on a solid SiC sample and on aqueous solution samples.

Silicon Carbide

Silicon carbide (SiC) is a crystalline solid that exhibits great physical, electrical and chemical properties. The tetrahedral crystalline covalent bonds are relatively strong. SiC is also well suited for use in radiation environments. Normal silicon in transistors or

semi-conductor devices has a mean time to failure of 10 years at 100°C, but SiC can survive for a similar time at 500°C (7). SiC promises to provide electronics that require less maintenance and are more durable in adverse environments. Its properties are being studied extensively for a wide variety of applications, including in such exotic uses as future fusion reactors (8).

SiC was not widely available until the late 20th century due to the difficulty of producing mass quantities of low defect material. As such, most research has been conducted on this material within the last decade.

There are many types of SiC. They can be categorized as cubic, hexagonal and rhombic. The letter C, H or R designates the type. A number precedes the type designator describing the stacking of layers within the crystal structure. This number-letter combination is known as Ramsdell notation. The two most common types are 4H and 6H SiC. The different types of SiC have similar, though not the same, positron lifetimes in bulk material and in defects (9).

Since SiC lends itself to use in high radiation environments, effects of fast neutron bombardment on the material are important. Neutrons lose energy in SiC through collisions. Since the neutron is not a charged particle, the influence of the electron cloud surrounding an atom is minimal, allowing the neutron to collide directly with the nucleus. These collisions may move an atom from its original location in the crystal lattice to a new point resulting in a vacancy and an interstitial atom. Another possibility is a distortion of the lattice resulting in a defect due to charge distribution. Defect clusters can form if the displaced atom has enough energy to displace other atoms from their location in the crystal structure. Defects can be removed by annealing at high

temperatures. Many studies have been done that examine the effect of annealing on irradiated SiC (7). Several studies have been done that examine the effects of neutron irradiation of SiC (10).
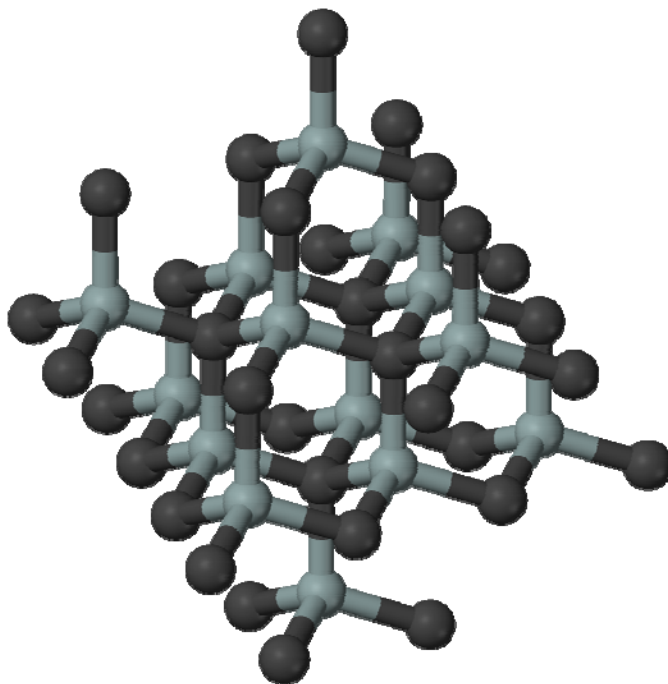
Figure 9. Crystalline structure of SiC.

Nitrates

The nitrate ion is composed of three oxygen atoms attached to a nitrogen atom, NO_3^-. Nitrates are a naturally occurring chemical essential to natural processes. Nitrates are commonly used in fertilizers.

Nitrates are also commonly used in explosives. The oxygen atoms provide essential material for the oxidation process which results in explosive energy release. Molecules having nitro groups as part of their molecular structure can be more efficient and faster burning explosives than hydrocarbons mixed with nitrates as in gunpowder.
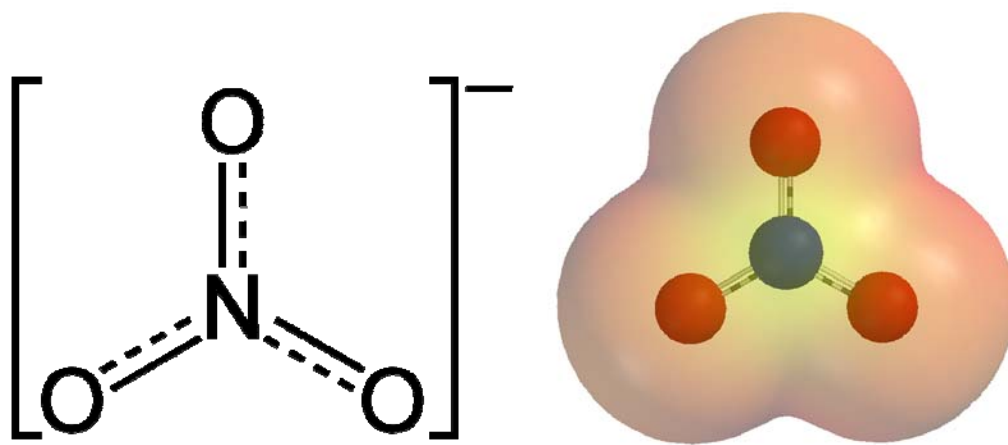
Figure 10. Resonance hybrid showing the bonds in the nitrate ion and an electrostatic potential map. Red areas show lower potential than the green.

III. Experimental Procedure

This section describes the electronic modules necessary for a timing application. It discusses the construction and optimization of the PALS system. Then it describes the sources used in the experiment.

Overview

I acquired a timing spectrum that is of better resolution and quality than what was collected on the fast-slow setup created by Capt Paul Adamson and described in his PhD dissertation (13). This was facilitated by high quality, lower noise photomultiplier tubes than were available for the fast-slow setup. A typical PALS setup is shown in Figure 11.
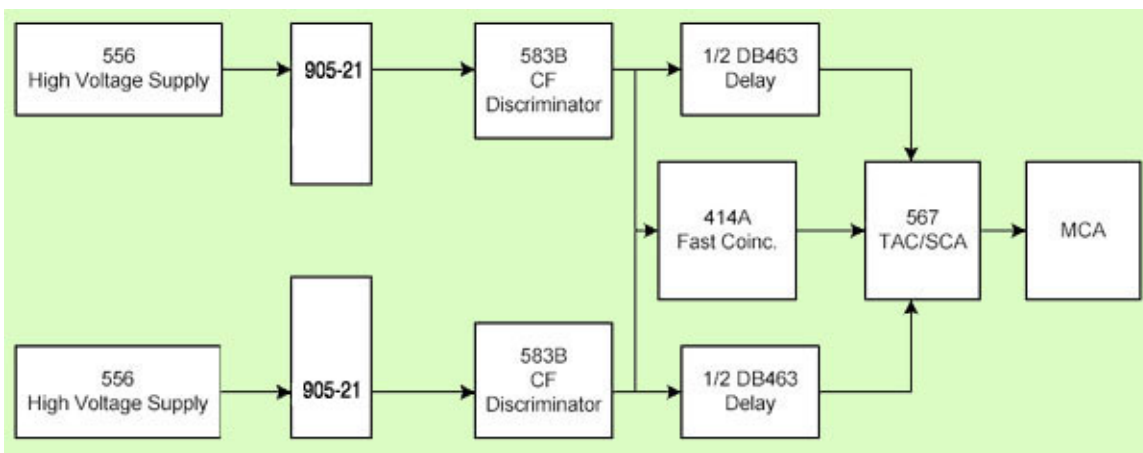
Figure 11. Fast-fast PALS.(11)

PALS Electronics

The detectors consist of a scintillator crystal made of barium fluoride, BaF_2 and a photomultiplier tube. BaF_2 has a very fast component in its scintillation decay (.7 ns) and a high atomic number which make it attractive for applications requiring both high

efficiency and fast response. The incoming gamma ray excites a molecular electron which emits a UV photon upon deexcitation (12). The BaF_2 scintillator is optically coupled to a Hamamatsu photomultiplier tube that changes the optical signal from the detector into an electronic current pulse via a photocathode coupled to an electron multiplier structure.

The crystal size on the start detector is 2x3 cm and the stop detector crystal size is 2x2 cm. The larger crystal size on the start detector is more efficient at capturing the higher energy gamma photons of the start pulse. Bias voltage was set to -2300 V on each detector.

The photomultiplier electronic signal is sent to a Constant Fraction Discriminator (CFD). The CFD multiplies and inverts the signal to generate a trigger at a predetermined fraction of the incoming pulse. This eliminates the walk error of a leading-edge type trigger, which adds uncertainty to the timing. The lower-level discriminator of the CFD receiving the signal from the start detector is set to accept pulses in the 1.274 MeV peak and ignore the pulses of lower energies. The stop detector pulses are discriminated in the same way, eliminating signals with energies lower than the 0.511 MeV peak.

A Fast Coincidence Unit (FCU) selects those pulses that occur within the selected time frame (initially set at 200 ps, then adjusted as necessary to obtain the best time resolution) indicating that they are a birth/annihilation photon pair. A Time-to-Amplitude Converter converts the signal into a timing spectrum which is sent to the laptop computer for analysis via a Multi-Channel Analyzer. The TAC window was set to 50 ns, the lowest available setting.

Finally, the PALSfit program deconvolves the timing spectrum into its component lifetimes. Typically about 10^6 annihilations need to be recorded to resolve the spectrum. PALSfit uses a least squares method to fit the measured spectrum to a sum of decaying exponentials.

The expected system resolution is less than 250 ps. Possible alterations to the setup may provide a better resolution. The use of Timing Single Channel Analyzers instead of the CFDs may provide better energy discrimination resulting in better timing resolution (12). Also, a logic module might be used in lieu of the FCU for better timing properties. There may also be another method of using the CFDs to better discriminate the energies so that the stop detector does not record a birth pulse. I attempted to optimize the system to provide the best possible timing resolution. A typical timing spectrum is shown in Figure 12.
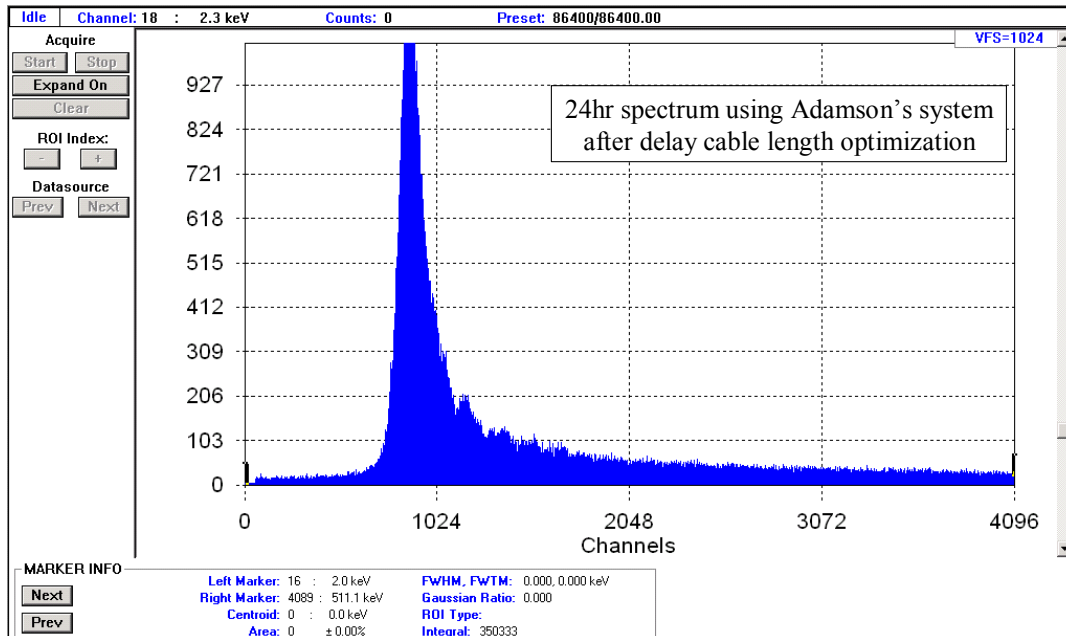
Figure 12. A typical PALS timing spectrum.(13)

System Setup and Optimization

To visualize the scales involved in PALS, consider that in a resolving time of 150 ps, light travels 0.5 cm, and a 5 μCi source produces 185,000 positrons per second. Gathering so many data points in such a short time requires the use of special electronics. The equipment, software and radioisotopes used in this research are listed in Appendix B.

Improving timing resolution allows a more accurate analysis of time spectra. There are many variables in the system that affect the timing resolution. The type of scintillator used, the photomultiplier tube (PMT) characteristics and the electronic modules all have an intrinsic electronic noise which degrades the resolution of the system. Setting up a PALS system requires iteratively improving settings to improve the timing resolution.

A ^{60}Co source was used to determine the timing resolution. ^{60}Co emits two gamma rays in its decay process at energies of 1332 and 1173 keV. These gammas are emitted nearly simultaneously and should produce a delta function on the timing spectrum. The inefficiencies and noise in the system result in a Gaussian distribution, the FWHM of which is the system timing resolution.

The time-per-channel was determined by running the output from a single CFD to the TAC start and stop inputs. The stop channel was sent through a delay box. The delay was increased by known amount. The time per channel at 8192 channels was determined to be 6.2 ps per channel, the same as the calculated value. Therefore, at this number of channels the FWHM needs to be under 33.3 channels for a resolution of 200 ps.
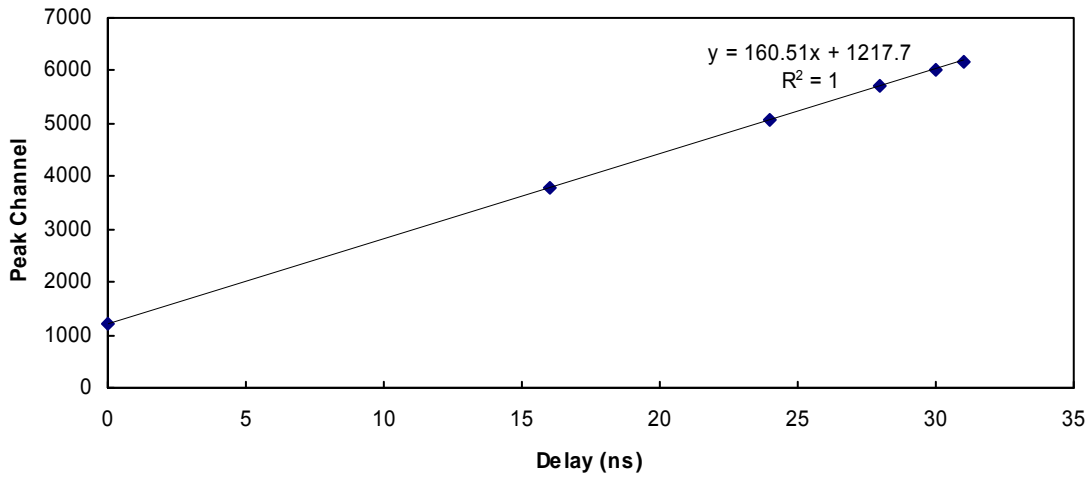
Figure 13. Calibration of Time per Channel. The fit is linear giving 6.2 ps per channel.

Relocation of the source from the side of the detector axis to a position between the two detectors greatly increased the count rate of the system due to improvement in the solid angle and did not appear to have an appreciable negative effect on the timing resolution. There was an anomalous peak in the timing spectrum, attributed to a reflected photon, which was eliminated by moving the detectors further apart.

Positioning the detector faces at 90° relative to each other appeared to improve the FWHM by about 10 percent. However, the count rate dropped by several orders of magnitude, negating the benefit to the timing resolution.

a. Source next to detectors

d. Detectors at 90°

b. Source between close detectors

c. Source between far detectors

e. Stop detectors in coincidence
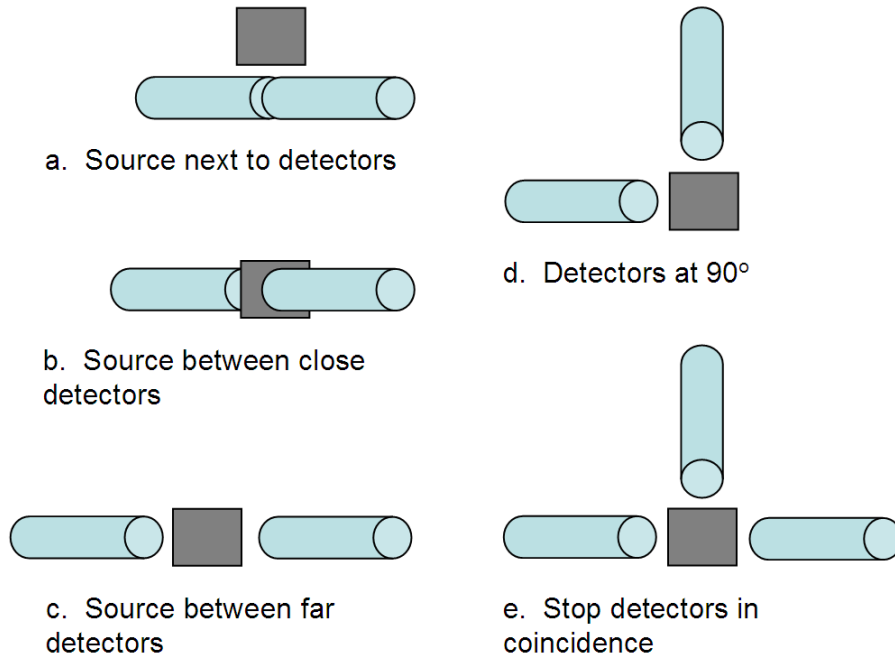
Figure 14. Various Detector Geometries.

An attempt was made at utilizing a third channel in the quad CFD to eliminate counts above the 0.511 MeV peak value. The input pulse from the stop detector was split into two CFD channels: one set below the 0.511 MeV peak and the other above. The two channels were then sent to the quad logic card which counted an event when the signal was on the first channel and not the second.

Another iteration of the three detector setup utilized two stop detectors in coincidence to provide the stop signal to the TAC. The third detector added substantial noise through the additional electronics which negated any benefit. The three detector setup also had a count rate several orders of magnitude below that of the two detector setup due to the decreased solid angle.

Methods to improve timing resolution included selection of window widths, walk voltages on the CFD, delay settings enroute to the TAC, detector geometry and possibly

interchanging the start and stop detectors. This latter method would probably not work for my setup since the two detectors are different sizes, to better capture different energy level gamma rays. According to Knoll (12), the FWHM should be between 5-10 channels to minimize electronic distortions in low count rates. This would dictate a width of 1024 channels which would result in a FWHM of 4.09 to give a resolution of 200 ps. However, I chose to use 8192 channels to maximize the resolution in the timing peak.

The CFD walk was adjusted in accordance with the operator's manual. Making this adjustment significantly improved the resolution, cutting the timing resolution from about 450 ps to 246 ps.

The cables connecting the modules needed to be 50 ohm cables for most of the connections. There was an odd reflection in the cable from the delay box to the TAC which was not resolved by changing cables or by adding in termination. The probable cause of the reflection is a tee connector which goes to the oscilloscope and the TAC. I removed the tee but then was unable to observe the pulse to verify if the reflection was eliminated.

A 10 ns delay is required between the gate pulse threshold and the start pulse threshold of the TAC input. Therefore, there is a minimum delay requirement for the start channel. Adjusting the delay on the stop channel to optimize the system led to the conclusion that the minimum delay possible should be used.

The delay cable length on the CFD is important. This cable sets the constant fraction to 20 percent of the pulse height. The formula provided in the user's manual

indicates the delay-cable length should be 0.3 m. The actual length of cable that gave

optimum results was 0.48 m.
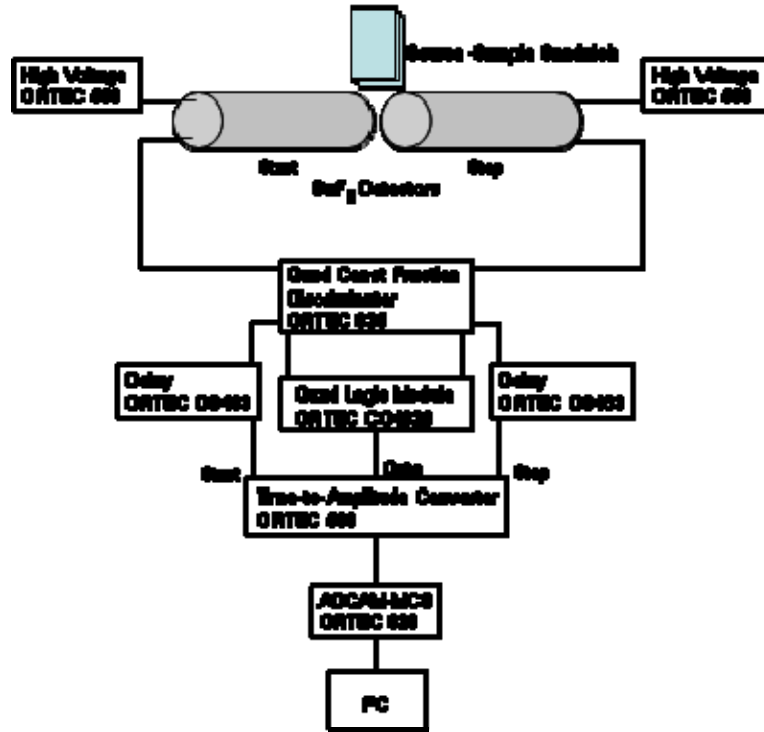
Figure 15. Fast-fast PALS system initial setup.

Values for timing resolution found in the literature vary greatly, from 300 ps to

150 ps. One fast PALS setup achieved a resolution of 140 ps by surrounding their system

with magnets to isolate from outside influences (14). They also constructed their own

PMTs and customized their CFDs. A digital system was reported to have a timing

resolution of 119 ps in 2001 (15).

A calculation showed the activity level of the source only allowed for one

positron in the sample at a time. This negated the need for the quad logic module.

Removing the quad logic module further reduced the electronic noise in the system and resulted in the final timing resolution of 197 ps.
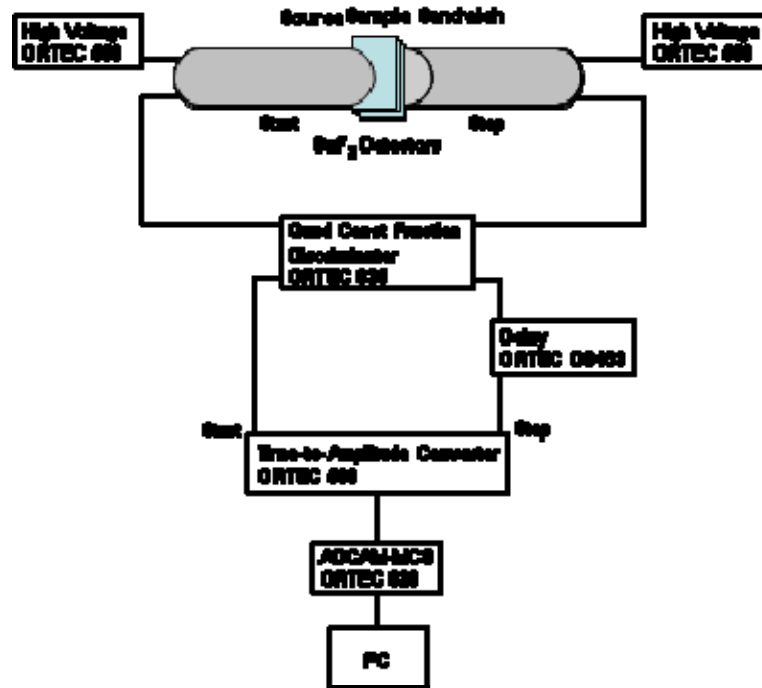
Figure 16. PALS system final geometry.

After timing resolution optimization, the system was setup for positron counting by setting the CFD windows back to the gamma ray energies emitted from ^{22}Na. Final settings on the components are listed in Appendix A.

Sample-Source Configuration

The thin-film positron source used for experiments with solids (AFIT source T112A) was previously made by Capt Paul Adamson by evaporating a ^{22}Na solution onto a Mylar film (13). This Mylar source is placed between two pieces of the sample material. This sample-source sandwich configuration gives the greatest chance of

positron interaction with the sample material while minimizing annihilations outside of the sample. The sample-source sandwich is placed between the start and stop BaF_2 detectors.

The source created by Capt Adamson did not exhibit any signs of leakage and so was judged to be viable for use with the solid samples, W and SiC. The activity was 6.02 μCi as measured using a HPGe detector on 17 October 2007.

The aqueous solutions for the nitrate and borane solutions were mixed in the chemistry lab following the procedure shown in Appendix D. They were made from a borane solution mixed with differing concentrations of potassium nitrate. The activity in each sample was intended to be about 5 μCi.

It is desirable to minimize the contribution to the timing spectrum of annihilations within the positron source itself. To do this the geometry of the container can be optimized. The surface-to-volume ratio should be minimized to reduce the chance the positrons will annihilate in the walls of the container. The optimum shape would be a sphere which has the smallest surface-to-volume ratio of any three dimensional shape. Since practical containers do not come in spherical shapes, we must choose the best available geometry. Several containers were considered with the best being a glass vial with 15 mL nominal capacity. The lid is a rubber septum secured by a crimp-on top, which has the advantage of preventing absorption of gases.

Due to the uncertainty in the measured volume of ^{22}Na added to each solution, and the differences in volume added to each solution, the activity needed to be determined in some way other than estimating volume added and multiplying by the activity per unit volume of source. To determine activity, a ^{22}Na calibration source

(T106) of known activity (.293 µCi) was measured in the PALS system to determine the count rate (3.94 cps). The sample activity was then calculated using the simple ratio

$$\frac{A_1}{\dot{c}_1} = \frac{A_2}{\dot{c}_2} \qquad (1.6)$$

where A is the activity and $\dot{c}$ is the count rate. As a check of the accuracy, and to guard against non-linearity in the counting system, the calculation was repeated for a higher activity source, T112A, whose activity was verified in an HPGe detector system. The results of both calculations were similar, as shown in Table 1.

Table 1. Solution Source Activity. Activity calculated with calibrated reference source T106 (0.293 µCi), and with T112A (6.02 µCi).

Concentration (M)	Activity$_{106}$ (µCi)	Activity$_{112A}$ (µCi)
0	5.60	5.52
5	4.47	4.41
0.5	3.66	3.61
0.1	1.67	1.65
0.01	0.68	0.67
5	4.22	4.16

One important consideration in developing a source is to ensure that there is no overlap of annihilations in the material which could lead to false stop signals in the PALS system. For a 6 µCi source, the average time between decays is 4.6×10^{-6} sec. The lifetime of the positrons in the material is three orders of magnitude lower. Therefore, it is concluded that there is only one positron in the material at a time, as desired.

Initially, the molar fraction of nitrates to water was intended to closely mimic the fraction of nitrates in trinitrotoluene (TNT) in order to maximize the applicability of the results of this study to use in explosives. This intention was later relaxed to allow for a

study of positron chemistry in aqueous solution as related to inhibition of positronium formation. The initial list of samples was modified during the injection of the ^{22}Na into the vials (See Appendix C) due to a lower volume of ^{22}Na than expected. The as-made solution samples are listed in Table 2.

Table 2. List of Solution Samples

Bottle No.	AFIT ID No.	Solvent	Solute	NO_3^- Concentration (M)
1	T112B	$H_2O + K_2B_{12}H_{12}$	none	0
2	T112C	$H_2O + K_2B_{12}H_{12}$	$NaNO_3$	5
3	T112D	$H_2O + K_2B_{12}H_{12}$	$NaNO_3$	0.5
4	T112E	$H_2O + K_2B_{12}H_{12}$	$NaNO_3$	0.1
6	T112F	$H_2O + K_2B_{12}H_{12}$	$NaNO_3$	0.01
9	T112G	H_2O	$NaNO_3$	5

Note: The borane concentration is 0.4 M in samples 1-6.

IV. Results and Analysis

This section presents the data obtained during the PALS construction and measurements. It presents a steady-state kinetics model of positron annihilation to describe the chemical processes in the solutions.

Time Resolution

The timing resolution of the system was determined to be 197 ps by directly measuring the FWHM of a ^{60}Co timing spectrum (See Figure 17) calculated by multiplying the FWHM of the spectrum, 31.84 channels, by the time per channel, 6.2 ps. ^{60}Co is used because it emits two gammas during its decay (1332 and 1173 keV) nearly simultaneously. This should result in a timing peak of a single channel. Any spread is caused by the timing resolution of the system.
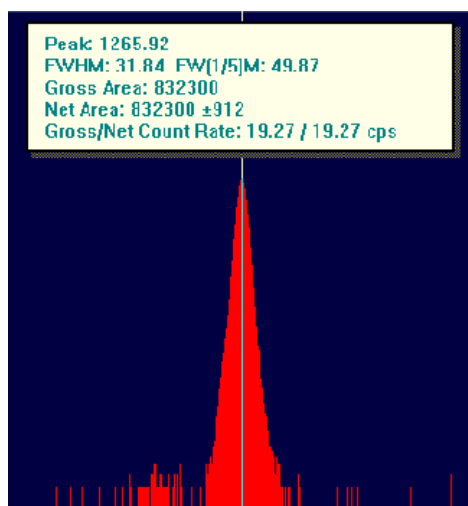
Figure 17. ^{60}Co timing spectrum.

All adjustable parameters involved have been optimized to reduce contributions to resolution uncertainties. Thus, it is hypothesized that the major remaining contributor to resolution inaccuracy is the detector/PMT combination.

PALSfit Software

Perhaps the most important aspect to PALS is the deconvolution of the spectra to determine the lifetimes present in the spectra. PALSfit is a program developed by the Riso National Laboratory in Denmark and is based on well-tested software. The program contains two modules: ResolutionFit and PositronFit. ResolutionFit determines the time resolution function of the PALS system while PositronFit extracts the lifetimes and intensities from the spectra using that resolution function. The model function consists of a sum of decaying exponentials convoluted with a resolution function, plus a constant background. The resolution function is a sum of Gaussians.

In ResolutionFit, an iterative process is used to determine the number of Gaussians and their intensities. This is the most time-consuming part of the process. The resulting resolution function is imported into PositronFit.

One important aspect of PositronFit is the ability to remove a source contribution. Source contributions from applicable materials are listed in Table 3.

PositronFit then outputs the calculated lifetimes and their standard deviations. Outputs also include a graph of the fitted spectrum and a residual plot.

Table 3. Positron Lifetimes Found in the Literature.

Material	τ_n (ns)	n
Mylar	1.82	3
Water	1.85	3
annealed Cu	0.112	2
SiC	0.142	2
Polyethylene	2.4	3
Tungsten	0.105	2
Plexiglass	1.9	3
^{22}NaCl	0.415	2
$K_2B_{12}H_{12}$	0.265	2

n is the lifetime indicator where n = 2 is free
positrons and 3 is ortho-positronium.
(References 5, 15, 16, 17)

Tungsten Sample

Measurement of the positron lifetime in tungsten (W) was used to determine the resolution function and verify the operation of the system. Tungsten is commonly used as a verification material since it has been well studied and has a well-defined bulk lifetime of 105 ± 5 ps (16). It also served as a way to learn the use of the PALSfit software.

The ^{22}Na source is sandwiched between the 5mm diameter tungsten crystals (100 plane). A timing spectrum was collected for 43200 seconds resulting in 1.69×10^6 counts.

PALSfit analysis of the spectrum gave a three Gaussian resolution function. The Gaussians were 0.2324, 0.5408 and 0.2113 ns FWHM with intensities of 77, 17 and 6%. The Gaussians were shifted from time zero by 0.0, 0.0690, and 0.1882 ns. The three intensities and the shift of the first Gaussian were fixed parameters. The tungsten spectrum is shown in Figure 18. PALSfit input parameters are listed in Appendix E.
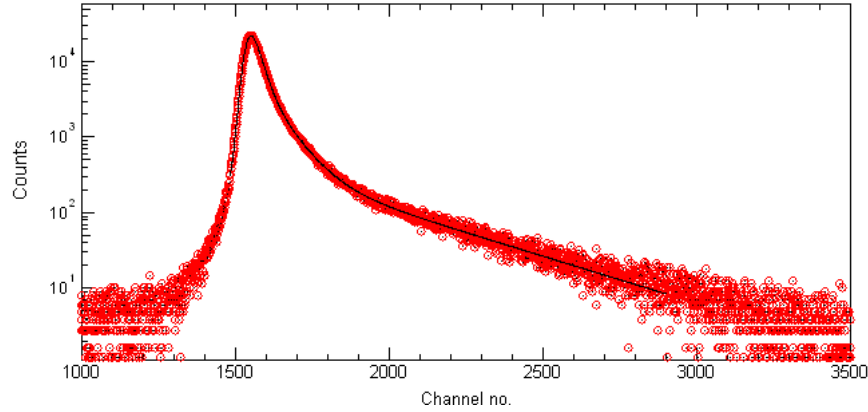
Figure 18. PALSfit Tungsten lifetime spectrum.

The ResolutionFit software looked for three lifetimes with τ_1, the bulk lifetime in tungsten, initially fixed at 105 ps. After an iterative process determined the proper resolution function, PositronFit was used to find the lifetimes in the crystal. The program removed the source contribution, 471 ps at 24.6% and 2.35 ns at 7.55%. The resulting two lifetimes were 101 ± 2 ps and 220 ± 11 ps with a variance of fit of 1.030. Corresponding intensities were 82.3% and 17.7%. The second lifetime is believed to be caused by vacancies within the crystal lattice. The value for the bulk lifetime is within the 105 ± 5 ps of published data, but the vacancy lifetime is slightly higher than the 195 ± 10 ps in the literature (16).

Silicon Carbide

Single crystal samples of 4H SiC were measured using the PALS system as a demonstration of the technique in analyzing a defected solid. Virgin samples were measured, then irradiated with a neutron fluence of 1×10^{13} n/cm^2 with > 0.5 MeV neutrons at the Ohio State University Nuclear Research Reactor. After irradiation, the samples were measured again, in the same configuration.

The SiC samples were measured pre-irradiation for 18000 seconds resulting in a PALS spectrum with 1.07×10^6 counts. The post-irradiation counting resulted in 1.36×10^6 counts in 18000 sec. The spectra were then analyzed using the PALSfit software. Pre- and post-irradiation spectra are shown in Figure 19. Residual plots are shown in Figure 20.
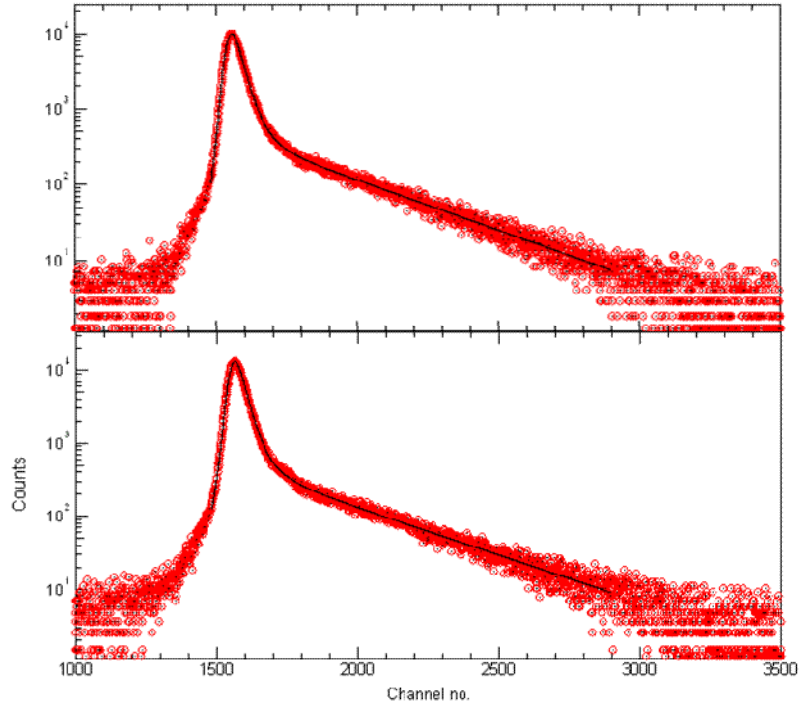
Figure 19. PALSfit spectra of pre- (top) and post-irradiated (bottom) SiC
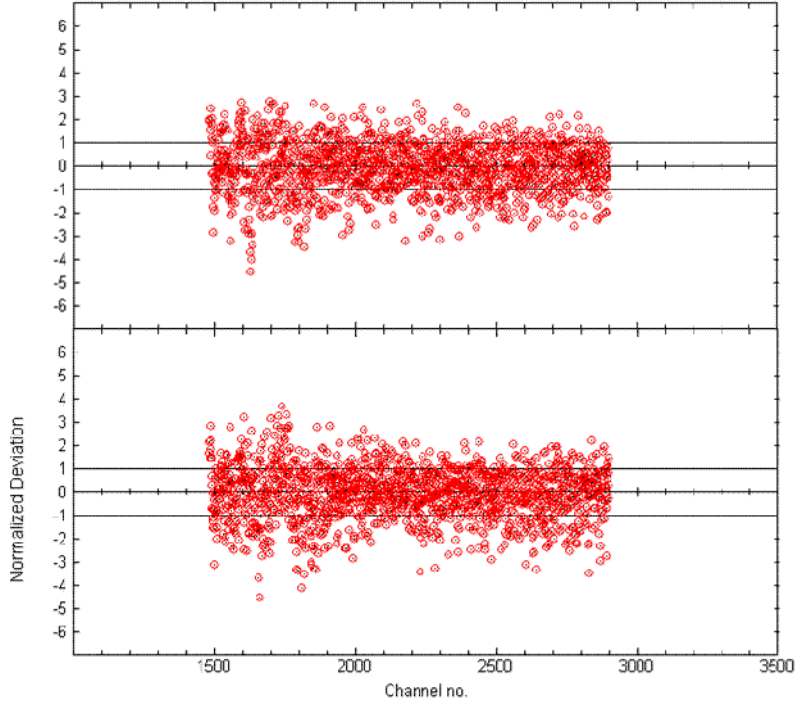
Figure 20. PALSfit residual plots of pre- (top) and post-irradiated (bottom) SiC.

Positron lifetime values for bulk SiC are given in the literature ranging from 134 – 150 ps. Vacancies are common in as-grown, or un-irradiated, SiC. Lifetime values for these vacancies are given in the range between 250 – 350 ps. A lifetime of 250 ps in SiC has been calculated to correspond to a vacancy of similar size to two missing silicon-carbon pairs, four atoms in all (17). Figure 21 shows the calculated positron lifetimes in vacancy clusters of a given size.

Using the PALSfit software, lifetimes were determined. In the un-irradiated sample, the bulk lifetime, τ_1, was determined to be 142 ± 3 ps and the defect lifetime, τ_2, was determined to be 298 ± 22 ps. Variance of the fit after source correction was 1.016. Both lifetimes are within the tolerance of published results.
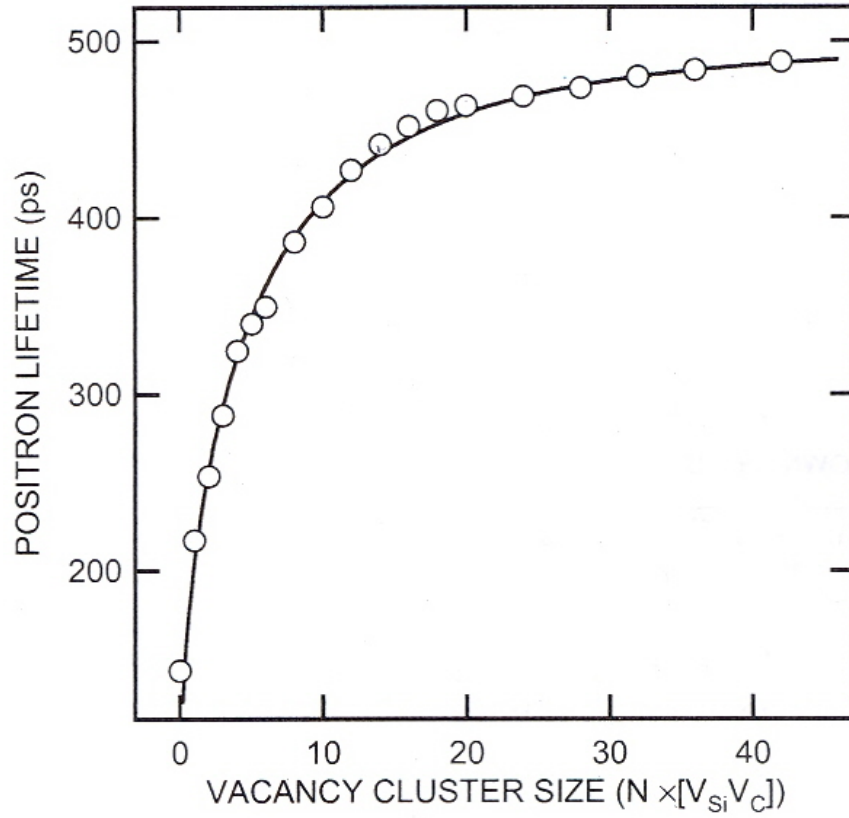
Figure 21. Calculated positron lifetimes in vacancy clusters in 4H SiC. (17)

After irradiation, the bulk lifetime increased to 148 ± 2 ps with the intensity increasing by 11% to 76%. This seems to indicate the presence of another, unresolved lifetime that is influencing the τ_1 result.

The silicon atom vacancies are more likely to attract positrons since carbon vacancies can be positively charged, and the resulting silicon vacancy has a positron lifetime on the order 195 ps. Carbon vacancies exhibit a lifetime of 160 ps (17). A calculation assuming one additional lifetime using

$$(\tau_1)(I_1) + (\tau_{unk})(I_{unk}) = (\tau_{tot})(I_{tot}) \tag{1.7}$$

where the subscript 1 represents the values in the virgin sample, gives the additional lifetime, τ_{unk}, of 201 ps with an intensity of 10.1 percent ($I_{tot} - I_1$). Therefore, it is concluded that the concentration of silicon vacancies has been increased by the neutron irradiation and that this is the primary contributor to the increase in bulk lifetime and its intensity.

The defect lifetime, τ_2, increased to 397 ± 35 ps. This value is expected for a vacancy cluster of the size of 10 missing silicon or carbon atoms (17). However, the decrease in intensity lends itself to the conclusion that the greatest effect of the neutron bombardment was to increase the number of silicon vacancies. Lifetimes of pre- and post-irradiated SiC are shown in Table 4.

Table 4. SiC Lifetimes and Intensities Before and After Irradiation.

Sample	τ_1 (ps)	I_1 (%)	τ_2 (ps)	I_2 (%)	τ_3 (ns)	I_3 (%)
Virgin	142 ± 3	64.6 ± 3.2	298 ± 22	16.9 ± 3.1	2.01 ± 0.01	18.4 ± 0.1
Irradiated	148 ± 2	75.7 ± 1.3	397 ± 4	8.6 ± 1.2	2.06 ± 0.02	15.8 ± 0.2

The third lifetime calculated in PALSfit is a convolution of source contributions from the Mylar ($\tau = 1.91$ ns) and plexiglass ($\tau = 2.0$ ns) surrounding the source. Its value, 2.01 ± 0.01 ns versus 2.06 ± 0.02 ns, was relatively constant with a small decrease in intensity, 2.7%, attributed to the increase in I_1. Variance of the fit post-irradiation was 1.061.

Nitrate Solution Samples

All the solution samples were measured for a length of time that allowed for capturing a spectrum with greater than 1×10^6 counts. Count times varied from 14400 sec to 111600 sec based on the activity of the samples. Spectra were analyzed using the

PALSfit software. The resolution function was determined by iteratively finding the best

fit to the data. It consisted of three Gaussians of the same intensity as the silicon carbide,

despite different sample geometry. This is not surprising as the detector setup was

exactly the same. The initial results are displayed in Table 5.

Table 5. Solution Sample Initial Results.

NO_3^- Concentration (M)	τ_1 (ns)	I_1 (%)	τ_2 (ns)	I_2 (%)	τ_3 (ns)	I_3 (%)
5	0.139 ± .009	12.7 ± 1.7	0.373 ± .007	83.6 ± .9	0.813 ± .094	3.6 ± 1.4
0.5	0.137 ± .005	27.6 ± 1.0	0.407 ± .004	62.7 ± .9	1.71 ± .02	9.7 ± .2
0.1	0.130 ± .005	24.5 ± .9	0.415 ±.006	58.5 ± .8	1.86 ± .03	16.9 ± .3
0.01	0.141 ± .006	25.1 ± 1.3	0.417 ± .008	54.6 ± 1.0	1.81 ± .03	20.3 ± .3
0	0.244 ± .002	71.8 ± 1.3	0.659 ± .083	9.3 ± .9	1.83 ± .03	18.9 ± .8
5 (no borane)	0.193 ± .005	34.9 ± 2.2	0.413 ± .006	64.7 ± 2.2	3.72 ± 3.71	0.4 ± .1

It can be noted that the samples containing 5M NO_3^- do not exhibit an easily

identifiable o-Ps lifetime as indicated by the τ_3 lifetime component varying greatly from

the τ_3 for o-Ps in water (1.81 ns). This is supported by the fact that NO_3^- is an electron

scavenger that at high concentration inhibits the formation of o-Ps by reducing the

availability of free electrons (18).

The most striking visualization of the o-Ps inhibition can be seen by comparing

the spectra of the sample that contained no NO_3^- to the sample with 5M NO_3^-. The

differences can be viewed in Figure 22. The o-Ps lifetime is manifested in the spectrum

as a long tail which is not present in the high concentration nitrate spectrum.
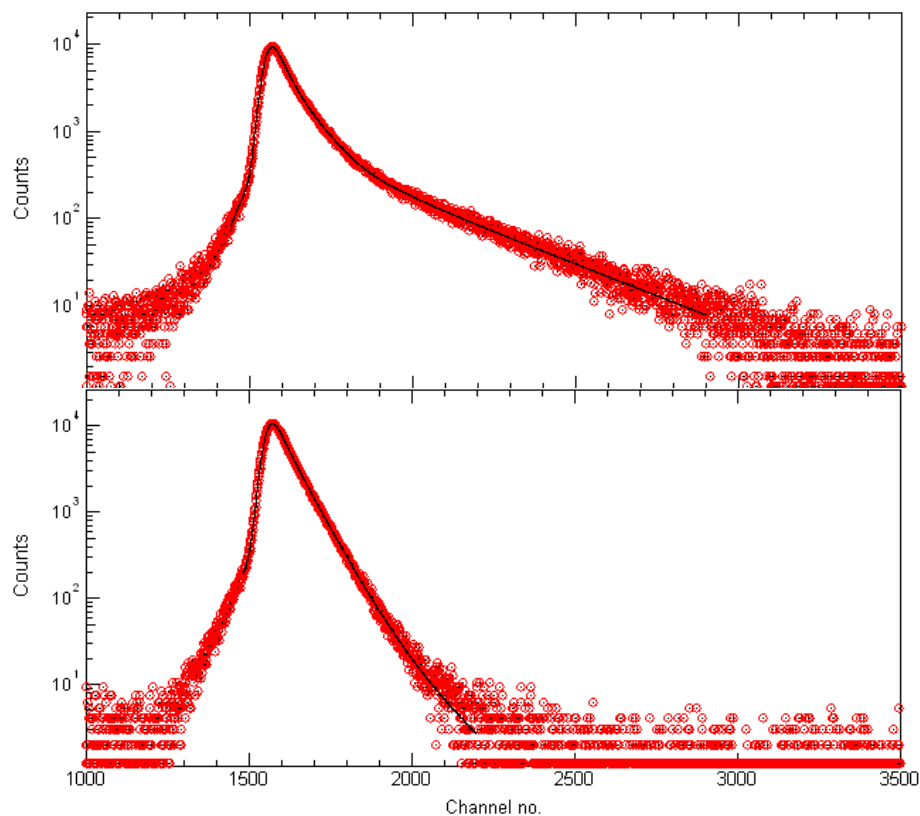
Figure 22. Ortho-positronium, shown by the long tail of the top figure (no NO$_3^-$), is absent in bottom figure (5M NO$_3^-$).

A second analysis using PALSfit, this time fixing the τ_3 component at 1.81 ns shows the decreasing intensity of the o-Ps component with the concentration of NO$_3^-$. The results are similar to published data (18).

Table 6. Intensity of the o-Ps (1.81 ns) lifetime component.

C(M)	$I_{1.81}$ (%)
5	0.55
0.5	8.83
0.1	17.4
0.01	20.5
0	19.8
5 (no borane)	-
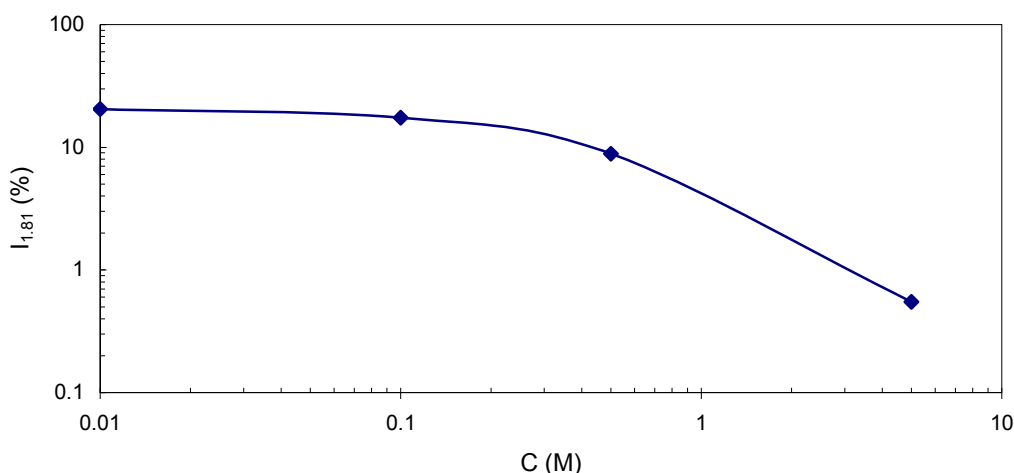
Figure 23. Variation of o-Ps intensity (%) at 1.81 ns with concentration of NO_3^- (M).

To determine the lifetime of positrons in the borane, it is noted that the 5M NO_3^- in borane solution result should be directly comparable to the 5M NO_3^- in water result, with any difference being attributable to the borane. By subtracting the τ_2 lifetime component seen in 5M NO_3^- in borane solution, 0.413 ns at 64.7 % intensity, from the 5M NO_3^- in water spectrum we see a residual lifetime in the spectrum of 0.277 ± 0.010 ns at 73.8% intensity. This lifetime is that associated with the borane. The resultant lifetime, 0.277 ± 0.010 ns, is similar to previous data taken on a solid sample (13). Capt Paul Adamson, in his research, obtained a positron lifetime of 0.2645 ± 0.0077 ns for $K_2B_{12}H_{12}$ with an intensity of 25.9 ± 0.3 %. Two additional lifetimes were obtained: 12.6651 ± 0.1872 ns and 1.9450 ± 0.0154 ns, with intensities of 20.2 ± 0.1 % and 53.9 ± 0.3 %, respectively, which were attributed to source contributions.

Applying this result to the data from T112B (no nitrate) gives lifetimes of:

$\tau_1 = 0.152 \pm 0.011$ ns (8.97%), τ_2 fixed at 0.277 ns (69.0%), $\tau_3 = 1.71 \pm 0.008$ ns (21.9%).

These values differ markedly from the original values because the PALSfit software was unable to resolve the τ_1 and τ_2 lifetimes without more parameters. The data suggests that the borane acts as a quenching mechanism for the o-Ps, reducing its lifetime (as opposed to inhibition which reduces intensity). For the other solutions, similarly fixing τ_2 at 0.277 ns in an effort to force the PALSfit software to find this lifetime only led to greatly degraded fits to the data as indicated by an increase in the variance of the fit. Therefore, I was unable to determine the intensity of the τ_2 lifetime component that was due to the decreasing nitrate concentration.

However, removing the source contribution, 0.413 ns, from the 0.5 M sample spectrum results in only two lifetimes of $\tau_1 = 0.138 \pm 0.002$ ns and $\tau_3 = 1.84 \pm 0.01$ ns. The other two spectra, 0.1 M and 0.01 M solutions, have a τ_2 too close to the source term to be deconvolved. These lifetimes indicate the presence of an unresolved fourth lifetime for a positron-nitrate bound state.

Table 7. Source Corrected Lifetimes and Intensities.

NO_3^- Concentration (M)	τ_1 (ns)	I_1 (%)	τ_2 (ns)	I_2 (%)	τ_3 (ns)	I_3 (%)
5 (source corrected)	0.122 ± .015	23.9 ± 6.0	0.277 ± .010	73.8 ± 5.8	1.81 ± .27	2.29 ± 0.28
0	0.152 ± .011	8.97 ± 1.07	0.277 (fixed)	69.0 ± 1.15	1.71 ± .01	21.9 ± 0.1
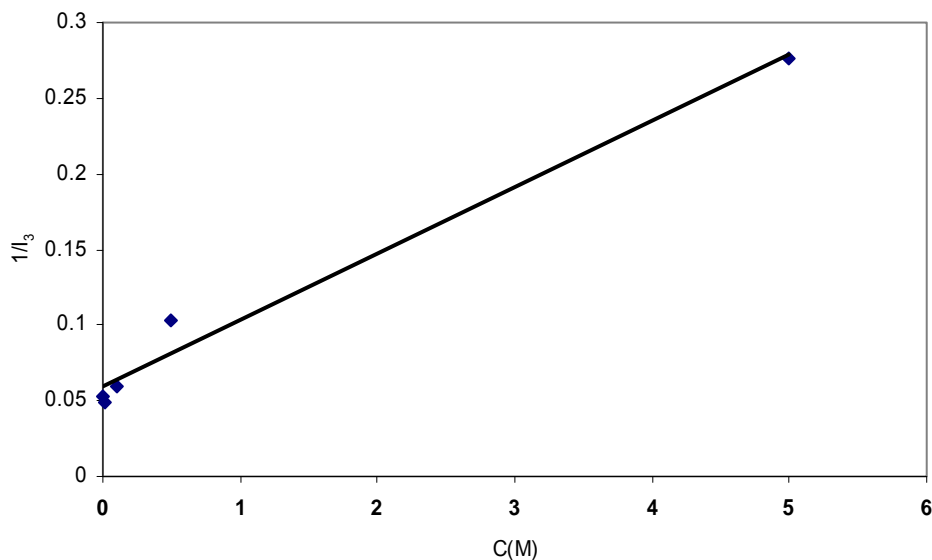
Figure 24. Variation of $1/I_3$ versus Concentration of NO_3^- and Linear Fit.

From the solution without nitrate $\tau_3 = 1.71 \pm 0.01$ ns. It appears that the borane serves to quench positronium formation, reducing its lifetime from 1.81 ns expected for water. This quenching effect is not seen in any subsequent solutions indicating that the quenching mechanism is eliminated by the presence of the nitrate. Another possibility is that the borane may have a somewhat shorter o-Ps lifetime than that for pure water and that the two are so close together that they remain unresolved.

Compared to previous experiments in which the o-Ps intensity, I_3^0, for pure water was determined to be 27.9% (18), the I_3 for the borane solution has a much reduced intensity, 19.8%. Therefore, there is an inhibiting effect as well as a quenching effect.

This indicates that some other process is at work. Several other processes can occur such as enhancement and partial inhibition (6). However, to fully characterize this relationship would require different concentrations of borane solution and the use of DBAR to determine the momentum of the positron.

A Steady State Model for Positron Annihilation

A steady state model (19) for the annihilation of positrons in nitrate/borane solution consists of the following interactions:

$$K \cdot R_{pf} = R_{ef}$$

$$e^+ + e^- \xrightarrow{k_{ep}} Ps \xrightarrow{k_{APs}} 2\gamma$$

$$e^+ + NO_3^- \xrightarrow{k_{pN}} NO_3^- \cdots e^+ \xrightarrow{k_{ApN}} 2\gamma$$

$$e^+ + B_{12}H_{12}^{-2} \xrightarrow{k_{pB}} B_{12}H_{12}^{-2} \cdots e^+ \xrightarrow{k_{ApB}} 2\gamma$$

$$e^+ + H_2O \rightarrow e^+ \cdots H_2O \xrightarrow{k_{ApW}} 2\gamma$$

$$Ps + NO_3^- \xrightarrow{k_{PsN}} e^+ + NO_2^- + O^-$$

$$e^- + NO_3^- \xrightarrow{k_{eN}} NO_2^- + O^-$$

$$e^- + H_2O \xrightarrow{k_{eW}} e^- \cdots H_2O$$
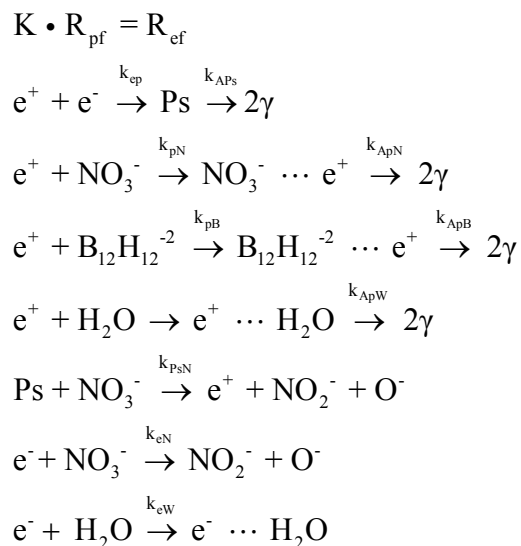
This model assumes homogeneity of the positron distribution. It also assumes that solvated electrons are removed from the population available to interact with positrons.

Activity, rather than concentration, is used in chemical calculations because solutions containing ionic solutes do not behave ideally in salt solutions and activity takes

into account the interaction of a molecule with its surroundings. The activity is proportional to the concentration (for constant ionic strength) but takes into account the interaction of ions in the solution. At very low concentrations the activity can be approximated by the concentration. However, at higher concentrations (> 0.1 M) the activity can be significantly different than the concentration. Therefore, the derivation of reaction rates is made more accurate by using activity in this case.

The Debye-Huckel equation is normally used to determine the unitless activity coefficient for low ionic strengths. However, the Davies approximation, a modification of the Debye-Huckel equation, is more valid for our purposes since we have a higher concentration (20). The Davies approximation is valid up to 0.5 M. The Davies approximation for the activity coefficient, γ, is

$$\log \gamma = -Az^2 \left(\frac{\sqrt{I}}{1 + \sqrt{I}} - 0.2\,I \right) \tag{1.8}$$

where A is a constant depending on the solvent (for water $A = 0.5$), z is the charge of the ion and I is the ionic strength given by

$$I = \frac{1}{2} \sum C_i z_i^2 \tag{1.9}$$

The activity is then calculated by

$$A = \gamma\,C \tag{1.10}$$

Using this formula, and data from (21) we get the unitless activity for the various nitrate concentrations as shown in Table 8.

Table 8. Nitrate Activity.

NO$_3^-$ (M)	I$_3$ (%)	Activity Coefficient, γ		Activity, [N]	I$_{3(}$0)/I$_3$
5	2.29	0.154	a	0.77	9.56
0.5	9.7	0.546	b	0.27	2.26
0.1	16.9	0.735	b	0.07	1.30
0.01	20.3	0.896	b	0.01	1.08
0	21.9	0		0.00	1.00

a Calculated using Davies Equation

b Data from (21).

Describing the positron steady state kinetics yields:

$$\frac{d[e^+]}{dt} = R_{pf} - k_{ep}[e^+][e^-] - k_{pA}[e^+][A^-] - k_{ApW}[e^+] = 0 \tag{1.11}$$

Where [ ] denotes activity and A represents the anion. Rearranging to solve for positron activity gives:

$$[e^+] = \frac{R_{pf}}{k_{ep}[e^-] + k_{pN}[N] + k_{pB}[B] + k_{ApW}} \tag{1.12}$$

Conducting a similar calculation for positronium activity results in:

$$[Ps] = \frac{k_{ep}[e^+][e^-]}{k_{APs} + k_{PsN}[N]} \tag{1.13}$$

Electron activity is likewise found to be:

$$[e^-] = \frac{K\,R_{pf}}{k_{ep}[e+] + k_{eN}[N] + k_{eW}} \tag{1.14}$$

Where K is a constant depending on the theory used (either 3 or 30). Note that the electron activity depends on the nitrate activity and the positron source activity. The

electron activity only depends on the borane activity indirectly through $[e^+]$, which is

small. Anion steady state kinetics are defined by:

$$[A \cdots e^+] = \frac{k_{pA}[e^+][A]}{k_{ApA}} \tag{1.15}$$

In analyzing the long lifetime component, we begin with:

$$k_{APs}[Ps] = k_{ep}[e_+][e_-] - k_{PsN}[Ps][N] \tag{1.16}$$

in which the second half is the correction for high nitrate activity. If we begin by

neglecting the nitrate correction and take the intensity of the long lifetime component as

the Ps annihilation rate over the rate of positron formation we get:

$$I_3 = \frac{k_{APs}[Ps]}{R_{pf}} = \frac{k_{ep}[e^+] K}{k_{ep}[e^+] + k_{eN}[N] + k_{eW}} \tag{1.17}$$

by substituting from (1.16) and (1.14).

The zero nitrate intensity is simply:

$$I_3^0 = \frac{k_{ep}[e^+] K}{k_{ep}[e^+] + k_{eW}} \tag{1.18}$$

We can now apply a Stern-Volmer type analysis by taking the ratio of (1.17) and (1.18)

resulting in:

$$\frac{I_3^0}{I_3} = 1 + \frac{k_{eN}[N]}{k_{ep}[e^+] + k_{eW}} \tag{1.19}$$

where I_3 is the intensity of the long lifetime component, I_3^0 is the intensity of the long

lifetime with no nitrate, k_{eN} is the rate constant for the oxidative scavenging of electrons

by the nitrate, $[N]$ is the activity of the nitrate, k_{ep} is electron-positron binding (or

positronium formation) rate, $[e^+]$ is the activity of the positrons, k_{eW} is the electron in

water solvation rate. Plotting this intensity ratio versus [N] should give a line with

intercept 1 and slope of $\dfrac{k_{eN}}{k_{ep}[e^+] + k_{eW}}$.
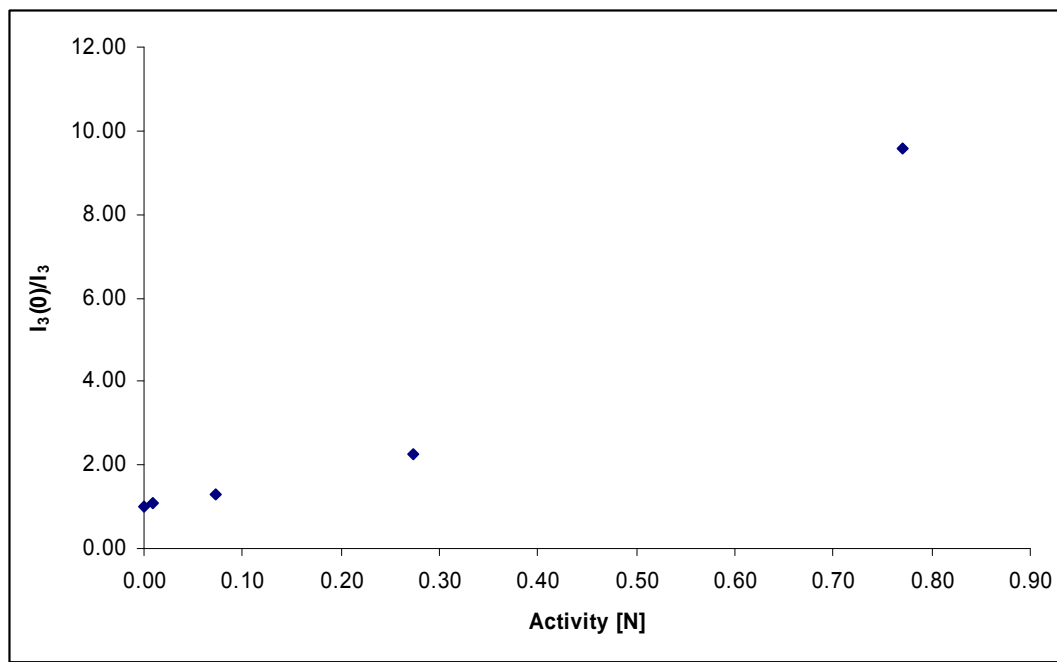
Figure 25. Intensity Ratio Versus Nitrate Activity.

This plot does deviate somewhat from linearity due to data uncertainty and the

breakdown of the Davies approximation above 0.5 M. Omitting the 5M data point,

which likely has the greatest uncertainty due to the inapplicability of the model at that

high of concentration, the trendline formula is $y = 4.5587x + 1.003$ with a fit of $R^2 =$

0.9969. The error of the model is determined by the error in the intercept value, .003.
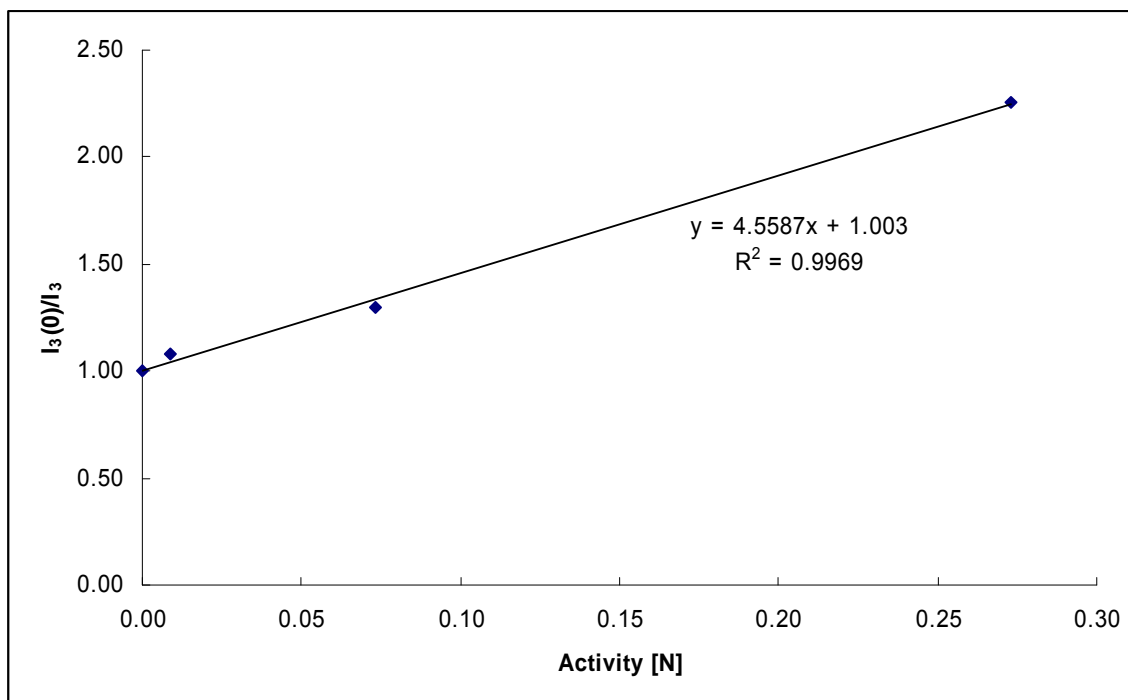
Figure 26. Linear Fit to Intensity vs Activity with 5 M data point removed.

Using the value of 0.24 ps for electron solvation (18) results in $k_{eW} = 4167$ ns^{-1} (or

0.4167×10^{13} s^{-1}) and k_{ep} [e$^+$] as 0.41 ns^{-1} we can estimate the value of $k_{eN} = 19000$ M^{-1}ns^{-1}

$(1.9 \times 10^{13}$ M^{-1}s^{-1}, as compared to 2×10^{13} M^{-1}s^{-1} found in the literature (18)). This reaction

rate indicates that electron scavenging takes place very rapidly, on the order of 5×10^{-14} s.

The above analysis neglects the oxidation of Ps by the nitrate ion (the high nitrate

concentration correction). If the oxidation is included, the intensity ratio becomes a

quadratic:

$$\frac{I_3^0}{I_3} = 1 + (a + b)[N] + ab[N]^2 \qquad (1.20)$$

Where a is the slope from the previous analysis:

$$a = \frac{k_{eN}}{k_{ep}[e^+] + k_{eW}}$$

and

$$b = \frac{k_{PsN}}{k_{APs}}$$

The chart shows a plot with y-axis labeled $I_3(0)/I_3$ (ranging 0.00 to 2.50) and x-axis labeled **Activity [N]** (ranging 0.00 to 0.30). The fitted curve is labeled:

$$y = 3.7079x^2 + 3.5147x + 1.0216$$
$$R^2 = 0.9989$$
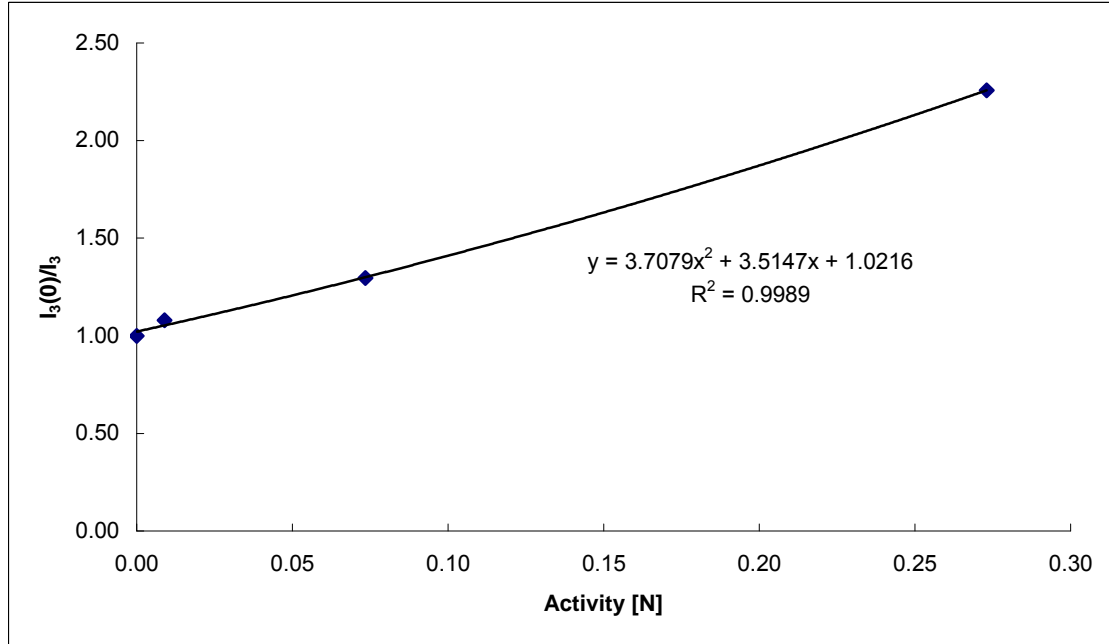
Attempts to solve (1.20) result in nonreal solutions. This indicates that Ps oxidation plays a very minor role, if any, in the inhibition of Ps. Rather, the Ps is prevented from forming in the first place by electron scavenging.

The analysis of the intermediate lifetime requires a slightly different approach. In this analysis we are assuming the intermediate lifetime is primarily due to positron interaction with the water. The $^{22}NaCl$ is also a contributor to this lifetime. The rate of annihilation, from (1.11) is:

$$k_{ApW}[e+] = R_{pf} - k_{ep}[e^+][e^-] - k_{pN}[e^+][N^-] - k_{pB}[e^+][B^-]$$
$$- k_{ApWL}[e^+] - k_{ApWS}[e^+] \tag{1.21}$$

where k_{ApWl} and k_{ApWs} represent the reaction rates for the longer and shorter components of annihilation of positrons in water, which account for the complex structure of water. The intermediate lifetime intensity is then:

$$I_2 = \frac{R_{pf} - k_{ep}[e^+][e^-] - k_{pN}[e^+][N^-] - k_{pB}[e^+][B^-] - k_{ApWL}[e^+] - k_{ApWS}[e^+]}{R_{pf}} \quad (1.22)$$

And the no nitrate intensity is similarly:

$$I_2^0 = \frac{R_{pf} - k_{ep}[e^+][e^-] - k_{pB}[e^+][B^-] - k_{ApWL}[e^+] - k_{ApWS}[e^+]}{R_{pf}} \quad (1.23)$$

In the Stern-Volmer type analysis, we would take the ratio of the intensities, however, this approach does not result in the intensity ratio versus slope equation as it did for the long lifetime component. Instead we take the difference between the intensities.

$$I_2 - I_2^0 = \frac{k_{pN}[e^+][N]}{R_{pf}} = \Delta I_2 \quad (1.24)$$

A plot of ΔI_2 versus [N] gives a linear relation with increasing nitrate activity.

57
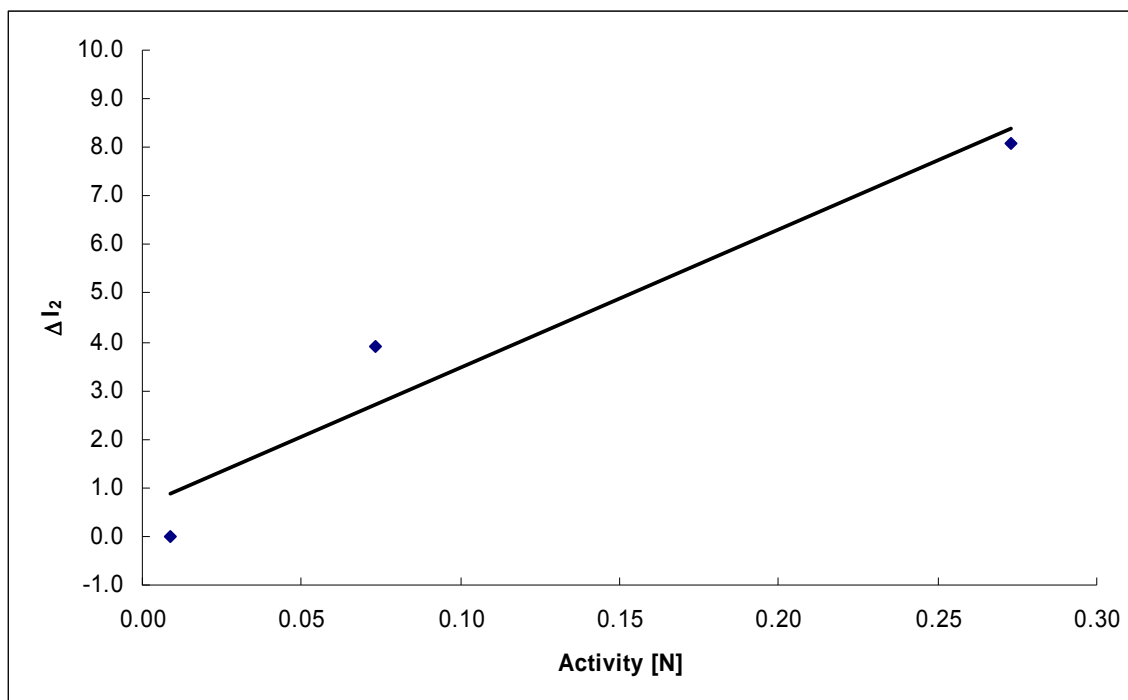
Figure 27. Change in Lifetime Intensity due to Activity.

This plot (Figure 27) shows the relation between the values, however, it should be noted that 0 M and 5 M solution values for I_2 were calculated using $I_2 = 0.277$ ns as opposed to a value closer to 0.413 ns that was calculated for the other three samples. A linear fit through the middle three data points gives a line $\Delta I_2 = 28.398[N] + 0.6353$. The intercept provides, which should cross at zero a means of evaluating the error of the method.

Evaluating the fitted slope with known values for k_{pN} and R_{pf} yields a value for the activity of the positrons as $[e+] = 0.00105$.

The short lifetime has contributions from nitrate and borane interactions with the positrons, as well as water species, such as OH^-, whose total short contribution is We^+. Assuming that all species are in steady state,

$$k_{pN}[e^+][N] = k_{ApN}[Ne^+]$$

$$k_{pB}[e^+][B] = k_{ApB}[Be^+]$$

$$k_{pW}[e^+][W] = k_{ApW}[We^+]$$

The positron annihilation rate becomes

$$R_1 = k_{ApN}[Ne^+] + k_{ApB}[Be^+] + k_{ApW}[We^+]$$

$$= k_{pN}[e^+][N] + k_{pB}[e^+][B] + k_{WS}[e^+][W]$$

The intensity is the short annihilation rate, R_1, divided by the total formation/annihilation rate R_{pf}.

$$I_1 = \frac{k_{pN}[e^+][N] + k_{pB}[e^+][B] + k_{WS}[e^+][W]}{R_{pf}} \tag{1.25}$$

and

$$I_1^0 = \frac{k_{pB}[e^+][B] + k_{WS}[e^+][W]}{R_{pf}} \tag{1.26}$$

Assuming that [e+] does not vary with experiment:

$$I_1 - I_1^0 = \frac{[e+]\, k_{pN}[N]}{R_{pf}} = \Delta I_1 \tag{1.27}$$

which indicates a linear increase with increasing [N]. The data does not support this conclusion which suggests that association of free e^+ with NO_3^- anions is weak.

Calculation of the reaction rate of positrons with the nitrate solution using

$$k_{ApN} = \frac{\ln(2)}{\tau_1} \tag{1.28}$$

gives $k_{ApN} = 3.59$ ns^{-1}. A similar calculation for the borane gives $k_{ApB} = 2.50$ ns^{-1}.

Table 9. Measured Reaction Rates.

Reation	Rate [ns^{-1}]	Nomenclature
$e^+ \cdots N \rightarrow 2\gamma$	3.59	k_{ApN}
$e^+ \cdots B \rightarrow 2\gamma$	2.50	k_{ApB}
$Ps \rightarrow 2\gamma$	0.41	k_{APs}
$e^+ \cdots H_2O \rightarrow 2\gamma$	1.68	k_{ApW}

V. Conclusions and Recommendations

Conclusions

The fast-fast PALS system worked as expected with a timing resolution of 197 ps as measured directly with a ^{60}Co source. Minimizing the number of electronic components in the system provided the best timing resolution by reducing the contribution of noise. The system succeeded in acting as a probe into the physical and chemical properties of solids and solutions.

The positron lifetime in single crystal tungsten was measured to be 101 ± 2 ps (as opposed to the published data of 105 ± 5 ps) with a monovacancy lifetime of 220 ± 11 ps. This data served to verify the operation and accuracy of the PALS system.

The PALS lifetime observed for silicon carbide exhibited evidence of forming silicon vacancies in the crystal lattice following neutron irradiation.

The aqueous nitrate anions inhibited the formation of ortho-positronium. Examination of the o-Ps intensities indicates that NO_3^- completely inhibits o-Ps formation with increasing concentration. The primary mechanism for Ps inhibition is electron scavenging, rather than oxidation of Ps. The borane is seen to reduce the effect of inhibition.

Recommendations for Future Work

Digitization of the PALS system should be the next step in improving AFIT's positron research. This step involves simply hooking the detectors directly up to a digitizer. The signal from the digitizer is directly analyzed by a computer. The hurdles

61

are hardware interface and programming the computer to perform all the tasks of the PALS.   Digitized PALS is the current state-of-the art.

Positron storage is an interesting field with practical importance for the future. A positron trap would allow for positron pulse analysis which will open up new avenues for the study of positron chemistry. This technology would enhance AFIT's ability to conduct detailed studies of materials. It is also a step on the pathway toward weaponizing antimatter.

Appendix A: Calculations

Adamson Source (T112A) Activity Verification		
300 sec count	Counts	
Adamson Source	8284342	
Calibrated Source	383870	
	Calibrated Source Activity	0.279
	Adamson Source Activity	6.02

Activity Required

Calibration Source	Calibration Date	Current Date	Time Difference [days]
T-106	15-Feb-03	17-Oct-07	1705

	Calibrated Activity [μCi]	Current Activity [μCi]	
	0.8883	0.293	

	Count Rate [cps]	Counts/(sec μCi)	Activity for 1E6 counts in 2 hr [μCi]
	8	27.34726617	5.078712002

	desired Count rate [cps]	Desired Activity	
	138.8888889	5.078712002	

5 mL of source
- 1 mL from Adamson
= 4 mL remaining

if I need .5 mL per source, I have enough 22Na for 8 sources

Calibrate Time Per Channel

Delay(ns)	Peak Channel	Time Difference	Peak difference	Time per channel		
0	1216	0	0	0		
16	3788	16	2572	0.00622084	6 ps per channel	
24	5071	8	1283	0.006235386	For a resolution of 200 ps, need a FWHM of	33.33333
28	5716	4	645	0.00620155		
30	6035	2	319	0.006269592		
31	6186	1	151	0.006622517		

If we take the TAC window, 50ns, and divide by the number of channels, 8192, we get 6.1 ps. This is a good approximation.

Start Channel Optimization

Stop Channel Optimization

Gate Optimization
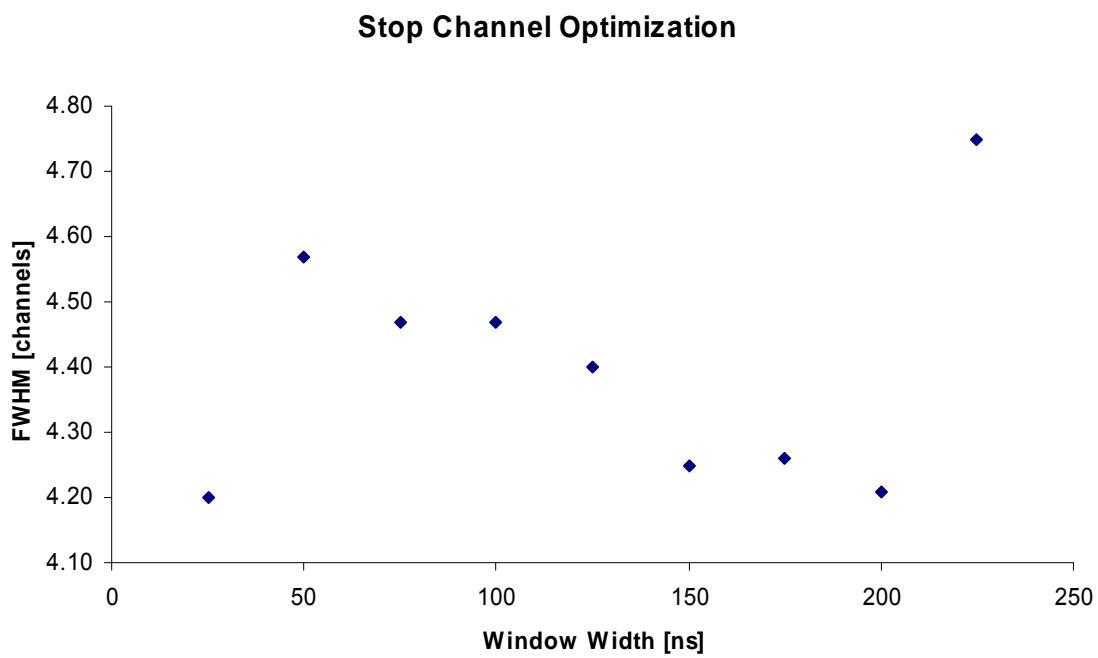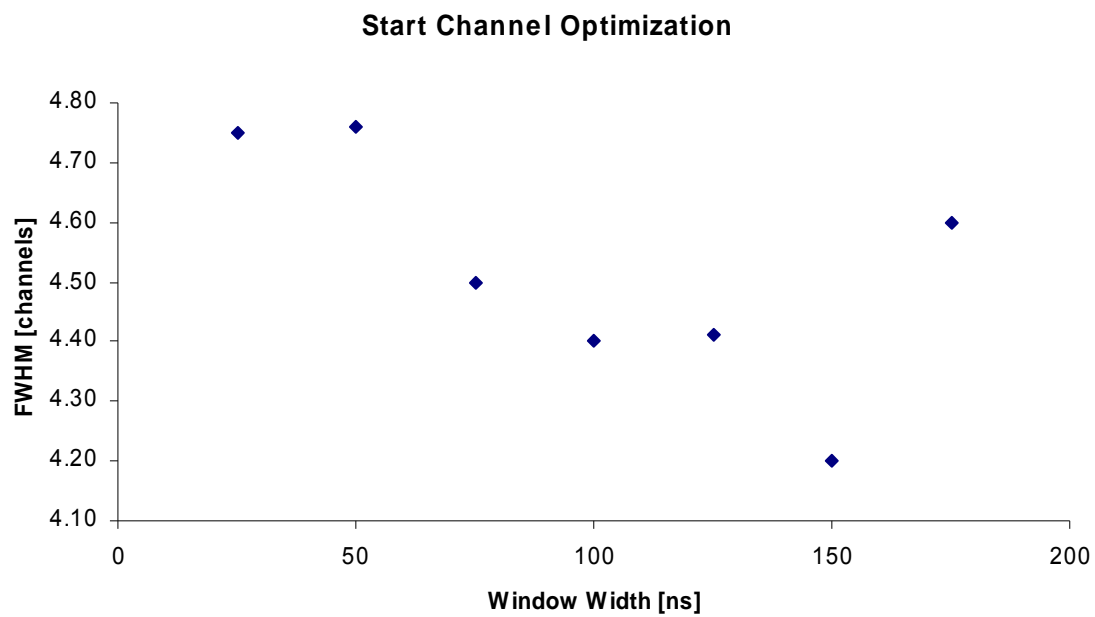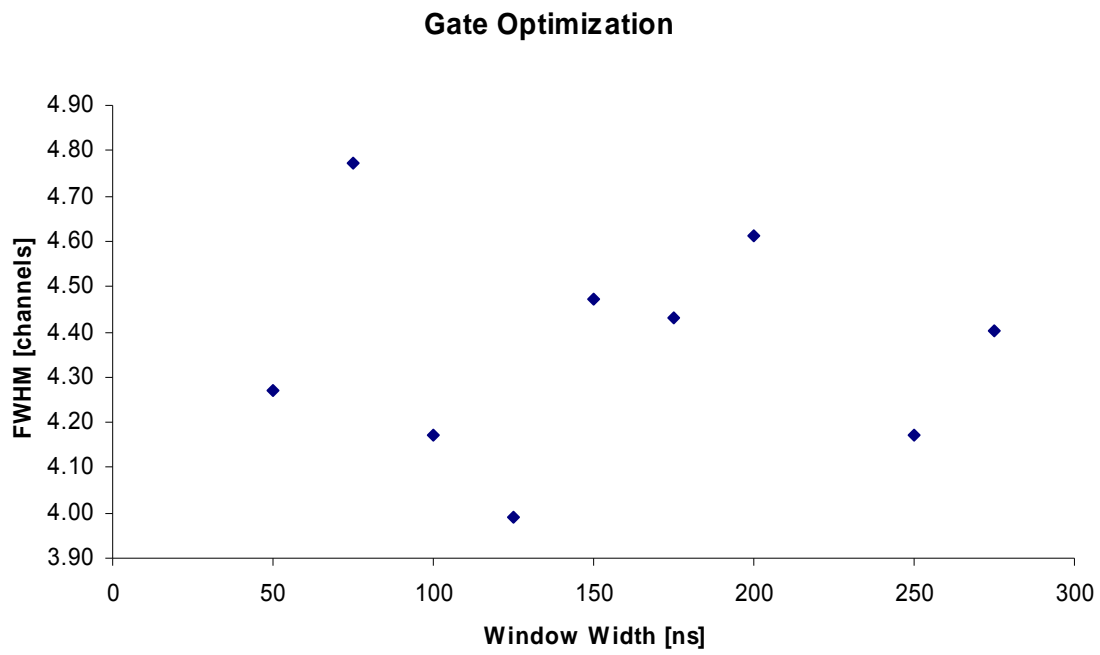
Appendix B: Equipment and Materials

Table 10. Equipment.

Laboratory Equipment	
Nomenclature	Model
HV Power Supply	Ortec 556
BaF2 detector/PMT	Saint Gobain/
Integrated module	Hamamatsu
Quad CFD	Ortec 935
Quad Logic	Ortec CO4020
FCU	Ortec 414A
TAC	Ortec 566
ADCAM/MCB	Ortec 926
Laptop	IBM ThinkPad
	Tektronix
Oscilloscope	TDS5104B

Table 11. Software.

Software		
Name	Version	Manufacturer
MAESTRO	6.04	AMETEK
PALSFit	1.16a	Riso Nat'l Labs

Table 12. Radioactive Sources.

Radiation Sources	
Type	Serial Number
Na-22	T-112A
Na-22	T106
Co-60	1U755

Appendix C: Procedure for Mixing Aqueous ^{22}Na Sources

Procedures for Preparing Aqueous ^{22}Na Solution Positron Sources

The following is a procedure for preparation of liquid ^{22}Na (as ^{22}NaCl) solutions by dilution of a stock ^{22}NaCl solution for use in positron spectroscopy, e.g. Positron Annihilation Lifetime Spectroscopy (PALS).

The sample preparation procedure will be conducted at the radiation hood in the radiochemistry lab in B470. Proper radiation safety and chemical safety procedures will be followed at all times.

1. Safety:

a. Personal Protective Equipment (PPE) will be worn at all times during this operation: disposable gloves (top two inches rolled down to allow removal without contaminating undergarments), lab coat, safety glasses.

b. At least two people will conduct the procedures, a primary operator and an assistant. The procedure will be conducted by the primary worker. The assistant will assist as necessary, e.g. if necessary the assistant can bring materials needed into the radiation hood after radioisotope transfer has begun so that there is little potential to bring contamination outside the hood.

c. Additionally, at least one radiation safety monitor will be present to verify the operation and to collect verification swipes.

c. All workers involved will wear TLDs, including a finger TLD.

d. Lead bricks will be used to minimize exposure to primary worker and assistant.

e. Radionuclide solution will be transferred from the radionuclide source

container to the sample containers using disposable syringe.

2. Procedure:

a. Setup

The setup is designed to minimize the amount of contaminated waste and to

minimize the risk of contamination outside the radiation hood. This will be accomplished

by the day prior to the sample transfer operation.

i. The radiation hood lab bench tops where radioactive material will be

handled will be covered with plastic sheeting taped down at corners. The plastic will be

covered by absorbent material. In the event of a radionuclide spill the plastic can be

wrapped around the paper and added to radiation waste container to prevent any

spreading of radiation.

ii. Prior to opening the radioactive source all materials will be laid out in

accordance with the planned setup shown in the diagram below.   All solutions except the

radionuclide source will be transferred into sample containers prior to opening the

radionuclide source solution.   The current ^{22}NaCl radionuclide solution is AFIT number

T-112 (4 g in 5 mL vial of 40 μCi ^{22}Na, 10 μCi /mL as of 1Dec07)

iii. A sign will be prepared for posting outside the door of the radiation

chemistry laboratory indicating that radioactivity is present and TLD is required for entry

during the preparation procedure; the sign will remain in place until the transfer and

cleanup is completed. A check will be made to ensure that radiation hazard signs outside

the radiation chemistry laboratory and on the radiation hood are in place.

Diagram of Setup

1   22Na Solution with Pb Shielding
2   Sample Container
3   22Na Container Lid
4   Syringe
5   Labels
6   Extra paper towels
7   Radioactive Waste Container
8   Work Area
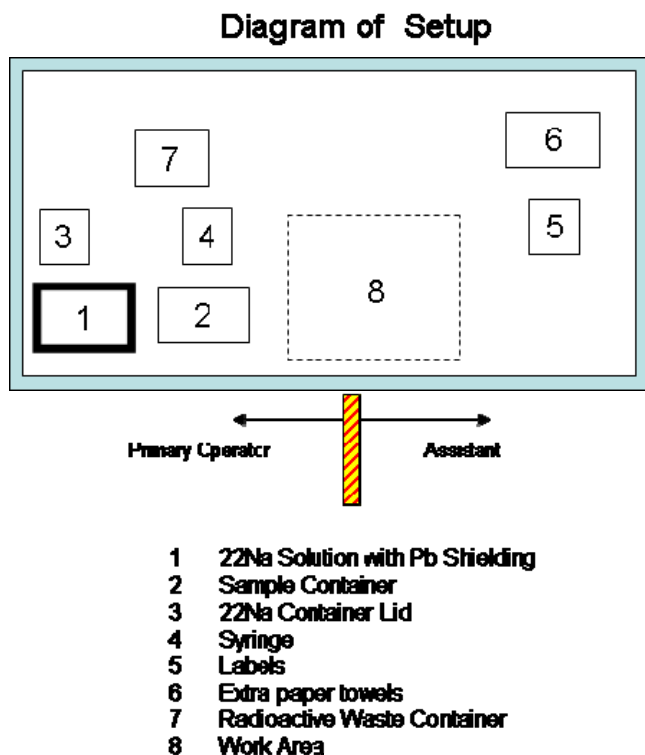
iv. A proof of concept container will be filled with tap water and sealed by

crimping using the procedure planned to seal sample containers. The sample bottle will

be injected with water. This will also give the primary operator practice using a syringe

prior to using the radioisotope source.

v. Sample solutions of non-radionuclide chemicals will be prepared ahead

of time with the appropriate concentration. Samples will be sealed by crimping.

vi. Prior to beginning the transfer procedure the volume of ^{22}NaCl solution

required to achieve the desired activity for each sample will be determined. For example,

using a stock solution of activity 10 μCi of ^{22}NaCl per mL at the time of procedure, to add 5 μCi of ^{22}NaCl to each sample container, 0.5 mL of stock solution would be added to each sample container.

vii. Labels for each sample container will be filled out ahead of time and applied to containers. All containers will be clearly identified and labeled with name of compound, radionuclide, date, ^{22}Na activity, and radiation type.

viii. Samples will be placed in a disposable sample holder.

b. Sample Preparation Operation

i. Personnel from 88 ABW/EMB Radiation Safety will be present to observe and advise during this procedure prior to opening the container of ^{22}NaCl stock solution and adding ^{22}NaCl to the sample containers.

ii. The volume of ^{22}Na radionuclide solution necessary to achieve the desired sample activity (usually 5-10 microcuries per sample) will be transferred from the source container to a sample container in a single syringe transfer. (All other non-radioactive solutions will have been previously added to this sample container.) This ^{22}Na transfer operation will be completed for each sample container. After all ^{22}Na transfers, the contaminated syringe will be immediately placed into the radiation waste container. The operator will seal the top of each container using silicon. The filled and sealed sample container will be set to the side in the sample container holder and shielded. The assistant will make measurements using a survey meter to preliminarily determine whether gross contamination exists. Then swipes will be taken. The results

will determine what cleaning and disposal procedures are necessary. The preliminary

sample preparation checklist is given in section 4 below.   The checklist will be modified

by the operator during practice, prior to transfer operations, to reflect the best procedure

that will minimize radioactive waste and minimize risk of radioactive spill.

4. Procedure Checklist:

    a. Setup

    □ Tape down plastic liner and locate absorbent

    □ Lay out sample container holder, sample containers, syringes, wipe test filter
papers, rad waste container.

    □ Label rad waste container with name of compound, radionuclide, date and
radiation type leaving a blank for ^{22}Na activity.

    □ Confirm non-radiation solutions have been added to sample containers

    □ Confirm labels on sample containers.

    □ Arrange all equipment except sources in the hood.

    □ Practice syringe use and sample sealing procedure.

    □ Ensure survey meters are operational

    □ Coordinate with machine shop personnel the time of planned transfer
operation.

    b. Transfer Operation

    □ Check, post signs

    □ Put on PPE

☐ Notify machine shop personnel of operation to bring ^{22}Na source into the radiation chemistry laboratory.

☐ Bring source solution from vault to radiation chemistry lab with assistant leading and monitor personnel following.

☐ Place ^{22}Na source in the radiation hood.

☐ Assistant hands sample containers to operator for ^{22}Na transfer.

☐ Operator remove lid from ^{22}Na source solution and place on filter paper.

☐ Measure total volume of ^{22}Na and divide by number of samples to determine exact amount to transfer to each sample.

☐ Carefully transfer aliquot of ^{22}Na solution into each sample container, ensure pressure in the sample is equalized or slightly negative prior to removing needle

☐ Place syringe into rad waste container

☐ Replace lid on ^{22}Na source solution.

☐ Use caulk gun to put silicon sealant on each sample

☐ Have assistant check operator's gloves and caulk gun for contamination using survey meter

☐ Swipe test all containers.

☐ Swipe tests will be conducted by 88 ABW/EMB Radiation Safety for all containers to ensure there is no radioactivity present on the outside of the sample containers or original source container.

☐ Repeat check of operator's gloves for contamination.

☐ Dispose of gloves and known contamination in rad waste.

☐ Conduct final cleanup after swipe analysis.

☐ Write the ^{22}Na activity on label for rad waste container.

☐ Place sample containers in individual container bags

☐ Check surface for contamination. Check the working surface with a gamma and beta counter for signs of radiation.

☐ All items will be swipe tested for contamination before disposal/removal from the table. If no contamination found, surface coverings will be left in place for possible future use.

☐ Check operator and assistant for contamination using survey meter.

☐ Move source and samples in container to room 107 lab via machine shop, with escort leading to open doors

☐ After removal of the source all items in the hood will be inspected by a hand held radiation detector to locate any significant contamination.

☐ Remove and discard PPE

☐ Check self for contamination again

☐ Wash hands

☐ Rad waste will be transferred to 88 ABW/EMB Radiation Safety for proper disposal immediately following completion of procedure and monitoring for contamination.

5. Accident procedures.

a. Prevent spreading of spill with paper towels.

b. Potentially contaminated PPE will be removed and measured for radiation prior to discarding.

b. Inform laboratory manager, Mr. Taylor and AFIT Radiation Safety Officer, Dr. Petrosky.

c. Clean spill area until contamination is below action level using instructions provided by AFIT Radiation Safety Officer.

6. Disposition.

a. Samples will be retained for use for up to 2 half lives (5 yrs) for possible follow on experiments.

b. Sources will be stored with multiple containment systems, impervious to the liquids contained inside (e.g., stainless steel or glass containers lined with absorbent paper).

b. When no longer needed, dispose of via sewer IAW 10 CFR 20 App B. Monthly avg concentration allowed: 6E-5 µCi/mL = 6E-2 µCi/L = 6 µCi/ 100 L.

Appendix D: Procedure for Preparing Aqueous Solutions

The aqueous nitrate solutions were created in the AFIT chemistry laboratory under the direction of Dr Feltcher. The first step, after determining requirements and initial lab familiarization, was to wash all the glassware to reduce the risk of outside contaminants affecting the PALS results.

The potassium dodecahydrodoedecaborate salt suffers a dearth of physical information. The manufacturer's website list the salt as being only 'slightly soluble' in water. Using this information as a guide, the salt was added to water slowly, at a rate of 0.5 g per 15 minutes of stirring. Eventually, the entire bottle of salt was added, totaling 97.4 g. The solution was allowed to stir and cool over night.

The next step was to mix the stock solutions by adding the nitrate in varying concentrations. The stock solutions were made by adding the masses shown below. The stock solutions were then diluted to make the sample solutions of the desired concentration.

	Stock solutions						
	Concentration (M)	mass (g)	vol (ml)	Dilute to	by adding	Dilute to	by adding
1 K2B12H12	0.46	97.38	1000	n/a			
2 NaNO3	5	42.5	100	n/a			
3 NaNO3	0.5	4.25	100	0.05	10mL	0.005	10mL
4 NaNO3	0.1	4.25	500	0.01	10mL	0.001	10mL
5 NaNO3 (in H2O)	5	42.5	100	n/a			

Once the solutions were mixed, they were bubbled with nitrogen for 15 minutes and transferred into the nitrogen purged glove box to prevent absorption of oxygen. Approximately 12 mL of each solution was then transferred into the sample vial. The

vial was sealed by crimping, labeled and placed in a storage container. ^{22}Na was added to

each vial as described in Appendix C.

Appendix E: PALSfit Output Files Showing Input Parameters and Results

Source Alone

```
R E S O L U T I O N F I T  VERS. AUG. 06 .  JOB TIME 16:43:38.12 25-DEC-07
****************************************************************************
7Nov inline tightened thresholds
****************************************************************************
TIME SCALE   NS/CHANNEL      :   0.006200
AREA RANGE   STARTS IN CH.   480 AND ENDS IN CH.   6200
FIT RANGE    STARTS IN CH.  1236 AND ENDS IN CH.   3000

INITIAL      FWHM (NS)       :    0.2324G    0.5408G    0.2113G
RESOLUTION   INTENSITIES (%) :   77.0000    17.0000     6.0000
FUNCTION     SHIFTS (NS)     :    0.0000F    0.0690G    0.1882G

OTHER INIT.  TIME-ZERO (CH.NO): 1290.7420G
PARAMETERS   LIFETIMES (NS)  :    0.1000G    0.4000G    1.8000G

BACKGROUND   FIXED TO MEAN FROM CH.   4000 TO CH.   6000   =        2.9785

##################### F I N A L  R E S U L T S #####################

CONVERGENCE OBTAINED AFTER   9 ITERATIONS
VARIANCE OF THE FIT =    1.044  WITH STANDARD DEVIATION 0.034
CHI-SQUARE = 1829.34  WITH 1753 DEGREES OF FREEDOM
SIGNIFICANCE OF IMPERFECT MODEL =  90.01 %
----------------------------------------------------------------------
RESOLUTION FUNCTION:                                           G  W  S
                                                               3  0  1
             FWHM (NS)       :    0.2286    0.6721    0.2657
             STD DEVIATIONS  :    0.0030    0.0322    0.0261

             INTENSITIES (%) :   77.0000   17.0000    6.0000

             SHIFTS (NS)     :    0.0000    0.0772    0.1493
             STD DEVIATIONS  :     FIXED    0.0171    0.0354
----------------------------------------------------------------------
LIFETIME COMPONENTS:                                           L  T  I
                                                               3  0  0
             LIFETIMES (NS)  :    0.1450    0.4713    2.3525
             STD DEVIATIONS  :    0.0079    0.0106    0.0244


             INTENSITIES (%) :   67.8329   24.6155    7.5516
             STD DEVIATIONS  :    1.2700    1.1884    0.1176
----------------------------------------------------------------------
TIME-ZERO    CHANNEL NUMBER  : 1291.1847
             STD DEVIATIONS  :    0.4497

TOTAL-AREA   FROM FIT    : 1.43550E+06        FROM TABLE : 1.44550E+06

SHAPE PARAMETERS FOR RESOLUTION CURVE (NSEC):
               N      2       5      10      30     100     300    1000
  FW    AT   1/N  0.2461  0.3935  0.5038  0.7445  1.1188  1.4026  1.6589
  MIDP  AT   1/N  0.0027  0.0101  0.0224  0.0603  0.0734  0.0734  0.0734

  PEAK POSITION IS IN CHANNEL # 1291.7921
##################### R E S O L U T I O N F I T #####################
```

Tungsten:

```
P O S I T R O N F I T . VERSION AUG. 06 . JOB TIME 15:02:53.93 03-JAN-08
****************************************************************************
27Nov 2ch 2cm inside bag
****************************************************************************
                                                        L  T  I  B  Z  A  G
                                                        3  0  0  1  1  0  3
TIME SCALE    NS/CHANNEL      :    0.006200
AREA RANGE    STARTS IN CH.   516 AND ENDS IN CH.  8192
FIT RANGE     STARTS IN CH.  1485 AND ENDS IN CH.  2900

RESOLUTION    FWHM (NS)       :     0.2324     0.5408      0.2113
FUNCTION      INTENSITIES (%) :    77.0000    17.0000      6.0000
              SHIFTS (NS)     :     0.0000     0.0690      0.1882

INITIAL       TIME-ZERO (CH.NO): 1537.6440F
PARAMETERS    LIFETIMES (NS)  :     0.1050G    0.4000G     1.8000G

BACKGROUND   FIXED TO MEAN FROM CH.   4000 TO CH.   7000    =        3.5072

----- R E S U L T S  B E F O R E  S O U R C E  C O R R E C T I O N -----
CONVERGENCE OBTAINED AFTER   5 ITERATIONS
CHI-SQUARE =   1411.71  WITH 1410 DEGREES OF FREEDOM
              LIFETIMES (NS)  :     0.1050     0.4116      2.1353
              INTENSITIES (%) :    61.2269    30.5351      8.2380
TIME-ZERO     CHANNEL NUMBER   : 1537.6440F
TOTAL-AREA    FROM FIT        : 1.70581E+06         FROM TABLE : 1.71353E+06

------------------- S O U R C E  C O R R E C T I O N -------------------
SOURCE        LIFETIMES (NS)  :     0.4710     2.3500
CORRECTION    INTENSITIES (%) :    24.6000     7.5500
              TOTAL (%)       :   100.0000

2ND CYCLE     LIFETIMES (NS)  :     0.1050G    0.2500G
PARAMETERS


##################### F I N A L  R E S U L T S #####################
                                                        L  T  I  B  Z  A  G
                                                        2  0  0  1  1  0  3
CONVERGENCE OBTAINED AFTER   6 ITERATIONS
VARIANCE OF THE FIT =     1.030  WITH STANDARD DEVIATION 0.038
CHI-SQUARE =   1454.39  WITH 1412 DEGREES OF FREEDOM
SIGNIFICANCE OF IMPERFECT MODEL =   78.88 %

              LIFETIMES (NS)  :     0.1010     0.2195
              STD DEVIATIONS  :     0.0015     0.0108

              INTENSITIES (%) :    82.3448    17.6552
              STD DEVIATIONS  :     2.4142     2.4142

BACKGROUND    COUNTS/CHANNEL  :     3.5072
              STD DEVIATIONS  :       MEAN

TIME-ZERO     CHANNEL NUMBER   : 1537.6440
              STD DEVIATIONS  :      FIXED
TOTAL-AREA    FROM FIT        : 1.16866E+06         FROM TABLE : 1.17377E+06

##################### P O S I T R O N F I T #####################
```

Silicon Carbide Pre-Irradiation:

```
P O S I T R O N F I T .  VERSION AUG. 06 .  JOB TIME 13:27:02.14 02-JAN-08
****************************************************************************
27 Nov 2ch SiC
****************************************************************************
                                                 L  T  I  B  Z  A  G
                                                 3  0  0  1  1  0  3
TIME SCALE    NS/CHANNEL      :    0.006200
AREA RANGE    STARTS IN CH.    487 AND ENDS IN CH.   8192
FIT RANGE     STARTS IN CH.   1485 AND ENDS IN CH.   2900

RESOLUTION    FWHM (NS)       :    0.2300     0.4264     0.0896
FUNCTION      INTENSITIES (%) :   74.0000    24.0000     2.0000
              SHIFTS (NS)     :    0.0000     0.0076    -0.0855

INITIAL       TIME-ZERO (CH.NO): 1542.5800F
PARAMETERS    LIFETIMES (NS)  :    0.1500G    0.2500G    1.8000G

BACKGROUND    FIXED TO MEAN FROM CH.   4000 TO CH.   7000    =       2.3582

----- R E S U L T S   B E F O R E   S O U R C E   C O R R E C T I O N -----
CONVERGENCE OBTAINED AFTER   6 ITERATIONS
CHI-SQUARE =    1408.77  WITH 1410 DEGREES OF FREEDOM
              LIFETIMES (NS)  :    0.1444     0.4186     1.9279
              INTENSITIES (%) :   51.5231    34.0615    14.4153
TIME-ZERO     CHANNEL NUMBER  : 1542.5800F
TOTAL-AREA    FROM FIT     : 1.06262E+06          FROM TABLE : 1.07076E+06

------------------ S O U R C E   C O R R E C T I O N -------------------
SOURCE        LIFETIMES (NS)  :    0.4710
CORRECTION    INTENSITIES (%) :   24.6000
              TOTAL (%)       :  100.0000

NORMAL CONTINUATION


##################### F I N A L   R E S U L T S #####################
                                                 L  T  I  B  Z  A  G
                                                 3  0  0  1  1  0  3
CONVERGENCE OBTAINED AFTER   7 ITERATIONS
VARIANCE OF THE FIT =     1.016  WITH STANDARD DEVIATION 0.038
CHI-SQUARE =    1432.73  WITH 1410 DEGREES OF FREEDOM
SIGNIFICANCE OF IMPERFECT MODEL =  66.94 %

              LIFETIMES (NS)  :    0.1420     0.2980     2.0098
              STD DEVIATIONS  :    0.0029     0.0224     0.0136

              INTENSITIES (%) :   64.6088    16.9727    18.4185
              STD DEVIATIONS  :    3.1515     3.0644     0.1488

BACKGROUND    COUNTS/CHANNEL  :    2.3582
              STD DEVIATIONS  :       MEAN

TIME-ZERO     CHANNEL NUMBER  : 1542.5800
              STD DEVIATIONS  :      FIXED
TOTAL-AREA    FROM FIT     : 8.07398E+05          FROM TABLE : 8.13826E+05

##################### P O S I T R O N F I T #####################
```

Silicon Carbide Post-Irradiation:

```
P O S I T R O N F I T .  VERSION AUG. 06 . JOB TIME 14:47:37.50 02-JAN-08
*************************************************************************
3Dec Irradiated SiC
*************************************************************************
                                                 L  T  I  B  Z  A  G
                                                 3  0  0  1  0  0  3
TIME SCALE    NS/CHANNEL         :     0.006200
AREA RANGE    STARTS IN CH.    475 AND ENDS IN CH.   8192
FIT RANGE     STARTS IN CH.   1485 AND ENDS IN CH.   2900

RESOLUTION    FWHM (NS)         :     0.2314     0.4775     0.1666
FUNCTION      INTENSITIES (%)   :    77.0000    17.0000     6.0000
              SHIFTS (NS)       :     0.0000    -0.0313    -0.0895

INITIAL       TIME-ZERO (CH.NO): 1549.3350G
PARAMETERS    LIFETIMES (NS)    :     0.1500G    0.3000G    1.9000G

BACKGROUND    FIXED TO MEAN FROM CH.   4000 TO CH.   7000    =        2.6488

----- R E S U L T S  B E F O R E  S O U R C E  C O R R E C T I O N -----
CONVERGENCE OBTAINED AFTER    8 ITERATIONS
CHI-SQUARE =    1493.37  WITH 1409 DEGREES OF FREEDOM
              LIFETIMES (NS)    :     0.1465     0.4431     1.9785
              INTENSITIES (%)   :    56.4130    31.3321    12.2549
TIME-ZERO     CHANNEL NUMBER    : 1551.0600
TOTAL-AREA    FROM FIT     : 1.35785E+06          FROM TABLE : 1.36799E+06

------------------- S O U R C E  C O R R E C T I O N -------------------
SOURCE        LIFETIMES (NS)    :     0.4710
CORRECTION    INTENSITIES (%)   :    24.6000
              TOTAL (%)         :   100.0000

NORMAL CONTINUATION


##################### F I N A L  R E S U L T S #####################
                                                 L  T  I  B  Z  A  G
                                                 3  0  0  1  0  0  3
CONVERGENCE OBTAINED AFTER    7 ITERATIONS
VARIANCE OF THE FIT =      1.061  WITH STANDARD DEVIATION 0.038
CHI-SQUARE =    1494.61  WITH 1409 DEGREES OF FREEDOM
SIGNIFICANCE OF IMPERFECT MODEL =   94.45 %

              LIFETIMES (NS)    :     0.1479     0.3972     2.0565
              STD DEVIATIONS    :     0.0019     0.0353     0.0165

              INTENSITIES (%)   :    75.6710     8.5563    15.7727
              STD DEVIATIONS    :     1.3286     1.2265     0.1686

BACKGROUND    COUNTS/CHANNEL    :     2.6488
              STD DEVIATIONS    :       MEAN

TIME-ZERO     CHANNEL NUMBER    : 1551.0282
              STD DEVIATIONS    :     0.0633
TOTAL-AREA    FROM FIT     : 1.03068E+06          FROM TABLE : 1.03899E+06

##################### P O S I T R O N F I T #####################
```

```
P O S I T R O N F I T .  VERSION AUG. 06 .  JOB TIME 10:18:28.85 05-JAN-08
**********************************************************************
T112B
**********************************************************************
                                              L   T   I   B   Z   A   G
                                              3   0   0   1   0   0   3
TIME SCALE   NS/CHANNEL      :   0.006200
AREA RANGE   STARTS IN CH.    454 AND ENDS IN CH.  8192
FIT RANGE    STARTS IN CH.   1445 AND ENDS IN CH.  2900

RESOLUTION   FWHM (NS)        :     0.2663     1.2251     0.4122
FUNCTION     INTENSITIES (%)  :    77.0000    17.0000     6.0000
             SHIFTS (NS)      :     0.0000     0.2614     0.1618

INITIAL      TIME-ZERO (CH.NO): 1548.6320G
PARAMETERS   LIFETIMES (NS)   :     0.1000G    0.3900G    1.8100G

BACKGROUND   FIXED TO MEAN FROM CH.   4000 TO CH.   7000    =      2.5921

----------------- N O   S O U R C E   C O R R E C T I O N ----------------

#################### F I N A L   R E S U L T S ####################
                                              L   T   I   B   Z   A   G
                                              3   0   0   1   1   0   3
CONVERGENCE OBTAINED AFTER  14 ITERATIONS
VARIANCE OF THE FIT =     1.040   WITH STANDARD DEVIATION 0.037
CHI-SQUARE =    1508.51   WITH 1450 DEGREES OF FREEDOM
SIGNIFICANCE OF IMPERFECT MODEL =   86.09 %

             LIFETIMES (NS)   :     0.2447     0.6594     1.8349
             STD DEVIATIONS   :     0.0024     0.0827     0.0314

             INTENSITIES (%)  :    71.7688     9.2859    18.9452
             STD DEVIATIONS   :     1.3314     0.8514     0.7638

BACKGROUND   COUNTS/CHANNEL   :     2.5921
             STD DEVIATIONS   :       MEAN

TIME-ZERO    CHANNEL NUMBER   : 1548.6320
             STD DEVIATIONS   :      FIXED
TOTAL-AREA   FROM FIT      : 1.07653E+06         FROM TABLE : 1.08368E+06

#################### P O S I T R O N F I T ####################
```

T112B Analyzed

```
P O S I T R O N F I T .  VERSION AUG. 06 . JOB TIME 14:57:55.35 19-FEB-08
**************************************************************************
T112B
**************************************************************************
                                              L  T  I  B  Z  A  G
                                              3  1  0  1  0  0  3
TIME SCALE   NS/CHANNEL      :   0.006200
AREA RANGE   STARTS IN CH.   454 AND ENDS IN CH.   8192
FIT RANGE    STARTS IN CH.  1445 AND ENDS IN CH.   2900

RESOLUTION   FWHM (NS)       :    0.2663    1.2251    0.4122
FUNCTION     INTENSITIES (%) :   77.0000   17.0000    6.0000
             SHIFTS (NS)     :    0.0000    0.2614    0.1618

INITIAL      TIME-ZERO (CH.NO): 1548.6320G
PARAMETERS   LIFETIMES (NS)  :    0.1000G   0.2770F   1.8100G

BACKGROUND   FIXED TO MEAN FROM CH.   4000 TO CH.   7000   =        2.5921

----------------- N O   S O U R C E   C O R R E C T I O N ----------------

##################### F I N A L   R E S U L T S #####################
                                              L  T  I  B  Z  A  G
                                              3  1  0  1  1  0  3
CONVERGENCE OBTAINED AFTER   9 ITERATIONS
VARIANCE OF THE FIT =    1.091   WITH STANDARD DEVIATION 0.037
CHI-SQUARE =   1582.80  WITH 1451 DEGREES OF FREEDOM
SIGNIFICANCE OF IMPERFECT MODEL =  99.15 %

             LIFETIMES (NS)  :    0.1523    0.2770    1.7060
             STD DEVIATIONS  :    0.0105     FIXED    0.0076

             INTENSITIES (%) :    8.9740   69.0371   21.9888
             STD DEVIATIONS  :    1.0698    1.1462    0.1145

BACKGROUND   COUNTS/CHANNEL  :    2.5921
             STD DEVIATIONS  :      MEAN

TIME-ZERO    CHANNEL NUMBER  : 1548.6320
             STD DEVIATIONS  :     FIXED
TOTAL-AREA   FROM FIT    : 1.07604E+06         FROM TABLE : 1.08368E+06

##################### P O S I T R O N F I T #####################
```

82

T112C Initial

```
P O S I T R O N F I T . VERSION AUG. 06 . JOB TIME 13:36:48.37 06-JAN-08
***************************************************************************
T112C
***************************************************************************
                                                         L  T  I  B  Z  A  G
                                                         3  0  0  1  0  0  3
TIME SCALE   NS/CHANNEL       :    0.006200
AREA RANGE   STARTS IN CH.    481 AND ENDS IN CH.   8192
FIT RANGE    STARTS IN CH.   1485 AND ENDS IN CH.   2200

RESOLUTION   FWHM (NS)        :    0.2955    0.2020    0.7518
FUNCTION     INTENSITIES (%)  :   77.0000   17.0000    6.0000
             SHIFTS (NS)      :    0.0000   -0.0368   -0.2136

INITIAL      TIME-ZERO (CH.NO): 1553.6340G
PARAMETERS   LIFETIMES (NS)   :    0.1000G   0.2000G   0.5000G

BACKGROUND   FIXED TO MEAN FROM CH.   4000 TO CH.   7000    =        2.2163

----------------- N O   S O U R C E   C O R R E C T I O N ----------------

##################### F I N A L   R E S U L T S #####################
                                                         L  T  I  B  Z  A  G
                                                         3  0  0  1  1  0  3
CONVERGENCE OBTAINED AFTER  15 ITERATIONS
VARIANCE OF THE FIT =    0.992  WITH STANDARD DEVIATION 0.053
CHI-SQUARE =     704.66  WITH  710 DEGREES OF FREEDOM
SIGNIFICANCE OF IMPERFECT MODEL =   45.05 %

             LIFETIMES (NS)   :    0.1396    0.3732    0.8138
             STD DEVIATIONS   :    0.0094    0.0070    0.0942

             INTENSITIES (%)  :   12.7377   83.6426    3.6197
             STD DEVIATIONS   :    1.6594    0.9049    1.4448

BACKGROUND   COUNTS/CHANNEL   :    2.2163
             STD DEVIATIONS   :      MEAN

TIME-ZERO    CHANNEL NUMBER   : 1553.6340
             STD DEVIATIONS   :     FIXED
TOTAL-AREA   FROM FIT    : 1.07694E+06       FROM TABLE :  1.08260E+06

##################### P O S I T R O N F I T #####################
```

83

T112C Analyzed

```
P O S I T R O N F I T .  VERSION AUG. 06 .  JOB TIME 15:00:45.85 19-FEB-08
**************************************************************************
T112C
**************************************************************************
                                                  L  T  I  B  Z  A  G
                                                  3  0  0  1  1  0  3
TIME SCALE    NS/CHANNEL      :    0.006200
AREA RANGE    STARTS IN CH.    481 AND ENDS IN CH.   8192
FIT RANGE     STARTS IN CH.   1485 AND ENDS IN CH.   2200

RESOLUTION    FWHM (NS)       :     0.2955    0.2020    0.7518
FUNCTION      INTENSITIES (%) :    77.0000   17.0000    6.0000
              SHIFTS (NS)     :     0.0000   -0.0368   -0.2136

INITIAL       TIME-ZERO (CH.NO): 1553.6340F
PARAMETERS    LIFETIMES (NS)  :     0.1000G   0.2000G   0.5000G

BACKGROUND   FIXED TO MEAN FROM CH.   4000 TO CH.   7000    =        2.2163

----- R E S U L T S  B E F O R E  S O U R C E  C O R R E C T I O N -----
CONVERGENCE OBTAINED AFTER  15 ITERATIONS
CHI-SQUARE =    704.66  WITH  710 DEGREES OF FREEDOM
              LIFETIMES (NS)   :     0.1396    0.3732    0.8138
              INTENSITIES (%)  :    12.7377   83.6426    3.6197
TIME-ZERO     CHANNEL NUMBER   : 1553.6340F
TOTAL-AREA    FROM FIT       : 1.07694E+06        FROM TABLE : 1.08260E+06

------------------ S O U R C E  C O R R E C T I O N -------------------
SOURCE        LIFETIMES (NS)   :     0.4130
CORRECTION    INTENSITIES (%)  :    64.7000
              TOTAL (%)        :   100.0000

NORMAL CONTINUATION


#################### F I N A L  R E S U L T S ####################
                                                  L  T  I  B  Z  A  G
                                                  3  0  0  1  1  0  3
CONVERGENCE OBTAINED AFTER   6 ITERATIONS
VARIANCE OF THE FIT =     0.992  WITH STANDARD DEVIATION 0.053
CHI-SQUARE =    704.12  WITH  710 DEGREES OF FREEDOM
SIGNIFICANCE OF IMPERFECT MODEL =   44.48 %

              LIFETIMES (NS)   :     0.1226    0.2768    1.8176
              STD DEVIATIONS   :     0.0148    0.0099    0.2701

              INTENSITIES (%)  :    23.9179   73.7879    2.2942
              STD DEVIATIONS   :     6.0169    5.8423    0.2813

BACKGROUND    COUNTS/CHANNEL   :     2.2163
              STD DEVIATIONS   :       MEAN

TIME-ZERO     CHANNEL NUMBER   : 1553.6340
              STD DEVIATIONS   :      FIXED
TOTAL-AREA    FROM FIT       : 3.92621E+05        FROM TABLE : 3.96883E+05

#################### P O S I T R O N F I T ####################
```

T112D Initial

```
P O S I T R O N F I T .  VERSION AUG. 06 .  JOB TIME 13:42:26.54 06-JAN-08
********************************************************************
T112D
********************************************************************
                                                L  T  I  B  Z  A  G
                                                3  0  0  1  0  0  3
TIME SCALE   NS/CHANNEL       :   0.006200
AREA RANGE   STARTS IN CH.    484 AND ENDS IN CH.  8192
FIT RANGE    STARTS IN CH.   1485 AND ENDS IN CH.  2900

RESOLUTION   FWHM (NS)        :    0.2527     0.6965     0.1732
FUNCTION     INTENSITIES (%)  :   77.0000    17.0000     6.0000
             SHIFTS (NS)      :    0.0000     0.0876     0.2117

INITIAL      TIME-ZERO (CH.NO):  1540.0000G
PARAMETERS   LIFETIMES (NS)   :    0.1000G    0.2000G    1.8100G

BACKGROUND   FIXED TO MEAN FROM CH.   4000 TO CH.   7000    =      1.7041

----------------- N O  S O U R C E  C O R R E C T I O N ----------------

#################### F I N A L  R E S U L T S ####################
                                                L  T  I  B  Z  A  G
                                                3  0  0  1  0  0  3
CONVERGENCE OBTAINED AFTER   9 ITERATIONS
VARIANCE OF THE FIT =    1.183   WITH STANDARD DEVIATION 0.038
CHI-SQUARE =    1667.11   WITH 1409 DEGREES OF FREEDOM
SIGNIFICANCE OF IMPERFECT MODEL = 100.00 %

             LIFETIMES (NS)   :    0.1366     0.4069     1.7107
             STD DEVIATIONS   :    0.0046     0.0044     0.0192

             INTENSITIES (%)  :   27.6212    62.7248     9.6540
             STD DEVIATIONS   :    1.0174     0.9052     0.1849

BACKGROUND   COUNTS/CHANNEL   :    1.7041
             STD DEVIATIONS   :     MEAN

TIME-ZERO    CHANNEL NUMBER   :  1541.9501
             STD DEVIATIONS   :    0.1000
TOTAL-AREA   FROM FIT     : 1.05394E+06        FROM TABLE : 1.06240E+06

#################### P O S I T R O N F I T ####################
```

T112 D Analyzed

```
P O S I T R O N F I T . VERSION AUG. 06 . JOB TIME 15:01:29.84 19-FEB-08
******************************************************************************
T112D
******************************************************************************
                                                   L  T  I  B  Z  A  G
                                                   2  0  0  1  0  0  3
TIME SCALE   NS/CHANNEL      :    0.006200
AREA RANGE   STARTS IN CH.    484 AND ENDS IN CH.   8192
FIT RANGE    STARTS IN CH.   1485 AND ENDS IN CH.   2900

RESOLUTION   FWHM (NS)       :    0.2527    0.6965    0.1732
FUNCTION     INTENSITIES (%) :   77.0000   17.0000    6.0000
             SHIFTS (NS)     :    0.0000    0.0876    0.2117

INITIAL      TIME-ZERO (CH.NO): 1540.0000G
PARAMETERS   LIFETIMES (NS)  :    0.1000G   0.2000G

BACKGROUND   FIXED TO MEAN FROM CH.   4000 TO CH.   7000    =        1.7041

----- R E S U L T S   B E F O R E   S O U R C E   C O R R E C T I O N -----
CONVERGENCE OBTAINED AFTER  19 ITERATIONS
CHI-SQUARE =    3839.24   WITH 1411 DEGREES OF FREEDOM
             LIFETIMES (NS)  :    0.3048    1.3504
             INTENSITIES (%) :   84.6079   15.3921
TIME-ZERO    CHANNEL NUMBER  : 1539.5214
TOTAL-AREA   FROM FIT        : 1.05122E+06          FROM TABLE : 1.06240E+06

------------------- S O U R C E   C O R R E C T I O N -------------------
SOURCE       LIFETIMES (NS)  :    0.4130
CORRECTION   INTENSITIES (%) :   64.7000
             TOTAL (%)       :  100.0000

NORMAL CONTINUATION


##################### F I N A L   R E S U L T S #####################
                                                   L  T  I  B  Z  A  G
                                                   2  0  0  1  0  0  3
CONVERGENCE OBTAINED AFTER   7 ITERATIONS
VARIANCE OF THE FIT =     1.289   WITH STANDARD DEVIATION 0.038
CHI-SQUARE =    1818.65   WITH 1411 DEGREES OF FREEDOM
SIGNIFICANCE OF IMPERFECT MODEL = 100.00 %

             LIFETIMES (NS)  :    0.1383    1.8370
             STD DEVIATIONS  :    0.0016    0.0106

             INTENSITIES (%) :   74.1681   25.8319
             STD DEVIATIONS  :    0.1746    0.1746

BACKGROUND   COUNTS/CHANNEL  :    1.7041
             STD DEVIATIONS  :      MEAN

TIME-ZERO    CHANNEL NUMBER  : 1544.1178
             STD DEVIATIONS  :    0.1523
TOTAL-AREA   FROM FIT        : 3.83954E+05          FROM TABLE : 3.90768E+05

##################### P O S I T R O N F I T #####################
```

T112E

```
P O S I T R O N F I T .  VERSION AUG. 06 .  JOB TIME 13:46:55.70 06-JAN-08
*********************************************************************
T112E
*********************************************************************
                                                    L  T  I  B  Z  A  G
                                                    3  0  0  0  0  0  3
TIME SCALE   NS/CHANNEL       :   0.006200
AREA RANGE   STARTS IN CH.   449 AND ENDS IN CH.   8192
FIT RANGE    STARTS IN CH.  1485 AND ENDS IN CH.   2900

RESOLUTION   FWHM (NS)        :     0.2498      0.6231      0.1721
FUNCTION     INTENSITIES (%)  :    77.0000     17.0000      6.0000
             SHIFTS (NS)      :     0.0000      0.0432      0.2046

INITIAL      TIME-ZERO (CH.NO): 1543.0000G
PARAMETERS   LIFETIMES (NS)   :     0.1000G     0.2000G     1.8100G


----------------- N O  S O U R C E  C O R R E C T I O N ----------------

#################### F I N A L   R E S U L T S ####################
                                                    L  T  I  B  Z  A  G
                                                    3  0  0  0  0  0  3
CONVERGENCE OBTAINED AFTER  10 ITERATIONS
VARIANCE OF THE FIT =    1.116  WITH STANDARD DEVIATION 0.038
CHI-SQUARE =   1571.83  WITH 1408 DEGREES OF FREEDOM
SIGNIFICANCE OF IMPERFECT MODEL =  99.86 %

             LIFETIMES (NS)   :     0.1303      0.4154      1.8582
             STD DEVIATIONS   :     0.0047      0.0055      0.0325

             INTENSITIES (%)  :    24.5433     58.4910     16.9657
             STD DEVIATIONS   :     0.9339      0.7638      0.2590

BACKGROUND   COUNTS/CHANNEL   :     0.3218
             STD DEVIATIONS   :     0.5743

TIME-ZERO    CHANNEL NUMBER   :  1543.8592
             STD DEVIATIONS   :     0.1024
TOTAL-AREA   FROM FIT     : 1.20359E+06        FROM TABLE : 1.22202E+06

#################### P O S I T R O N F I T ####################
```

87

T112F

```
P O S I T R O N F I T .  VERSION AUG. 06 .  JOB TIME 13:49:22.84 06-JAN-08
**************************************************************************
T112F
**************************************************************************
                                                        L  T  I  B  Z  A  G
                                                        3  0  0  0  0  0  3
TIME SCALE   NS/CHANNEL       :   0.006200
AREA RANGE   STARTS IN CH.   480 AND ENDS IN CH.   8192
FIT RANGE    STARTS IN CH.  1471 AND ENDS IN CH.   2900

RESOLUTION   FWHM (NS)        :     0.2453     0.6219     0.1652
FUNCTION     INTENSITIES (%)  :    77.0000    17.0000     6.0000
             SHIFTS (NS)      :     0.0000     0.0627     0.1882

INITIAL      TIME-ZERO (CH.NO): 1544.0000G
PARAMETERS   LIFETIMES (NS)   :     0.1000G    0.2000G    1.8100G


----------------- N O  S O U R C E  C O R R E C T I O N ----------------

##################### F I N A L  R E S U L T S #####################
                                                        L  T  I  B  Z  A  G
                                                        3  0  0  0  0  0  3
CONVERGENCE OBTAINED AFTER   9 ITERATIONS
VARIANCE OF THE FIT =    1.097  WITH STANDARD DEVIATION 0.038
CHI-SQUARE =    1559.59  WITH 1422 DEGREES OF FREEDOM
SIGNIFICANCE OF IMPERFECT MODEL =  99.40 %

             LIFETIMES (NS)   :     0.1410     0.4170     1.8087
             STD DEVIATIONS   :     0.0057     0.0075     0.0312

             INTENSITIES (%)  :    25.1276    54.6060    20.2664
             STD DEVIATIONS   :     1.2628     1.0378     0.3324

BACKGROUND   COUNTS/CHANNEL   :     0.6785
             STD DEVIATIONS   :     0.5301

TIME-ZERO    CHANNEL NUMBER   :  1544.5685
             STD DEVIATIONS   :     0.1062
TOTAL-AREA   FROM FIT      : 1.00884E+06        FROM TABLE : 1.01528E+06

##################### P O S I T R O N F I T #####################
```

T112G

```
P O S I T R O N F I T . VERSION AUG. 06 . JOB TIME 10:55:42.10 05-JAN-08
*****************************************************************************
T112G
*****************************************************************************
                                                    L  T  I  B  Z  A  G
                                                    3  0  0  1  0  0  3
TIME SCALE   NS/CHANNEL       :   0.006200
AREA RANGE   STARTS IN CH.    483 AND ENDS IN CH.  8192
FIT RANGE    STARTS IN CH.   1485 AND ENDS IN CH.  2200

RESOLUTION   FWHM (NS)        :     0.2693     0.7184     0.1512
FUNCTION     INTENSITIES (%)  :    77.0000    17.0000     6.0000
             SHIFTS (NS)      :     0.0000     0.0686    -0.0702

INITIAL      TIME-ZERO (CH.NO): 1543.3410G
PARAMETERS   LIFETIMES (NS)   :     0.1000G    0.2000G    0.5000G

BACKGROUND   FIXED TO MEAN FROM CH.   4000 TO CH.   7000    =      2.3605

----------------- N O  S O U R C E  C O R R E C T I O N ----------------

#################### F I N A L  R E S U L T S ####################
                                                    L  T  I  B  Z  A  G
                                                    3  0  0  1  1  0  3
CONVERGENCE OBTAINED AFTER  18 ITERATIONS
VARIANCE OF THE FIT =    0.995  WITH STANDARD DEVIATION 0.053
CHI-SQUARE =     706.10  WITH  710 DEGREES OF FREEDOM
SIGNIFICANCE OF IMPERFECT MODEL =  46.58 %

             LIFETIMES (NS)   :     0.1939     0.4133     3.7248
             STD DEVIATIONS   :     0.0052     0.0062     3.7124

             INTENSITIES (%)  :    34.9103    64.6840     0.4056
             STD DEVIATIONS   :     2.1824     2.1687     0.0352

BACKGROUND   COUNTS/CHANNEL   :     2.3605
             STD DEVIATIONS   :        MEAN

TIME-ZERO    CHANNEL NUMBER   : 1543.3410
             STD DEVIATIONS   :       FIXED
TOTAL-AREA   FROM FIT      : 1.11779E+06        FROM TABLE : 1.12345E+06

          #################### P O S I T R O N F I T ####################
```

89

Bibliography

[1] P.A.M. Dirac, Proc. Cambridge Phil. Soc., 26 1930, 91.

[2] Carl D. Anderson, *The Positive Electron*. Physical Review. 43, 1933, 491.

[3] Devanarayanan, P.E. *A Report on Setting Up of a Positron Lifetime Spectrometer*. Indira Gandhi Centre for Atomic Research, Kalpakkam. 2004.

[4] Davis, William C. *High Explosives, the Interaction of Chemistry and Mechanics*. Los Alamos Science. 2, 1. 48-75. 1981.

[5] Lazzarini, Ennio. *An Attempt to Apply Ligand Field Theory to Positronium Reactions with 3d Complexes*. Rend. Fis Acc Lincei 9, 14. 2003.

[6] Duplatre, Maddock, Abbe, Haessler. *The Chemistry of Positronium. IV. Quests on the Inhibition of Positronium in Aqueous Solutions*. Chemical Physics 28. 433-440. 1978.

[7] Bonavita, Angelo. *Low Temperature Hall Measurements of Neutron Irradiated Silicon Carbide*. Masters Thesis. Air Force Institute of Technology. 2004.

[8] Chen, Jung, Klein. *Production and recovery of defects in SiC after irradiation and deformation*. Journal of Nuclear Materials. 258-263. 1998.

[9] Lam, Lam, et al. *Positron Lifetime Studies on 8 MeV Electron-Irradiated n-type 6H Silicon Carbide*. Journal of Physics: Condensed Matter. 16, 8409-8419. 2004.

[10] Jones, Kent. *Measurement of Neutron Induced Surface and Bulk Defects in 4H Silicon Carbide*. Masters Thesis. Air Force institute of Technology. 2002.

[11] www.orteconline.com

[12] Knoll, Glenn F. *Radiation Detection and Measurement*. 3rd Ed. John Wiley and Sons. 2000.

[13] Adamson, Paul. *A General Quantum Mechanical Method to Predict Positron Spectroscopy*. AFIT Dissertation. 2007.

[14] Becvar, Cizek, et al. *A High Resolution BaF$_2$ Positron Lifetime Spectrometer and Experience with its Long-term Exploitation*. Nuclear Instruments and Methods in Physics Research A. 443, 557-577. 2000.

[15] Saito, Nagashima, et al. *A New Positron Lifetime Spectrometer Using a Fast Digital Oscilloscope and BaF$_2$ Scintillators*. Nuclear Instruments and Methods in Physics Research A. 487, 612-617. 2002.

[16] Robles, Ogando, Plazaola. *Positron Lifetime Calculation for the Elements of the Periodic Table*. Journal of Physics: Condensed Matter. 19, 176-222. 2007.

[17] Aavikko, Reino. *Positron Lifetime Spectroscopy: Digital Spectrometer and Experiments in SiC*. PhD Dissertation. Helsinki University of Technology, Finland. 2006.

[18] Jean, Mallon, Schrader Eds. *Positron and Positronium Chemistry*. World Scientific. 2003.

[19] Burggraf, Larry. Personal Communication. Jan 2008.

[20] Stum, Morgan. *Aquatic Chemistry, Chemical Equilibria and Rates in Natural Waters*. 3rd ed. Wiley. 1996.

[21] Lide, David, Ed. *CRC Handbook of Chemistry and Physics*. 84th Edition. CRC Press. 2003.

REPORT DOCUMENTATION PAGE

1. REPORT DATE *(DD-MM-YYYY)*	2. REPORT TYPE	3. DATES COVERED *(From - To)*
27-03-2008	Master's Thesis	June 2007- March 2008

4. TITLE AND SUBTITLE	5a. CONTRACT NUMBER
DEVELOPMENT AND OPTIMIZATION OF A POSITRON ANNIHILATION LIFETIME SPECTROMETER TO MEASURE NANOSCALE DEFECTS IN SOLIDS AND BORANE CAGE MOLECULES IN AQUEOUS NITRATE SOLUTIONS	5b. GRANT NUMBER
	5c. PROGRAM ELEMENT NUMBER

6. AUTHOR(S)	5d. PROJECT NUMBER
Matthew A. Ross MAJ, USA	5e. TASK NUMBER
	5f. WORK UNIT NUMBER

7. PERFORMING ORGANIZATION NAME(S) AND ADDRESS(ES)	8. PERFORMING ORGANIZATION REPORT NUMBER
Air Force Institute of Technology Graduate School of Engineering and Management (AFIT/EN) 2950 Hobson Way WPAFB, OH 45433-7765	AFIT/GNE/ENP/08-M05

9. SPONSORING/MONITORING AGENCY NAME(S) AND ADDRESS(ES)	10. SPONSOR/MONITOR'S ACRONYM(S)
Air Force Institute of Technology Graduate School of Engineering and Management (AFIT/EN) POC: Larry W. Burggraf 2950 Hobson Way WPAFB, OH 45433-7765	AFIT
	11. SPONSOR/MONITOR'S REPORT NUMBER(S)

12. DISTRIBUTION/AVAILABILITY STATEMENT

APPROVED FOR PUBLIC RELEASE; DISTRIBUTION UNLIMITED

13. SUPPLEMENTARY NOTES

14. ABSTRACT

A Positron Annihilation Lifetime Spectroscopy (PALS) system was developed and tested. PALS has the capability to characterize negatively charged defects and voids in materials such as explosives. The timing resolution of the optimized system is 197±14 ps as measured with a known 60Co source. A single-crystal tungsten sample was used to confirm the system calibration resulting in a lifetime of 101±2 ps (as compared to 105 ±5 ps in the literature (16)). The PALS system was then used to compare the differences between as grown and neutron-irradiated single crystal silicon carbide (SiC), illustrating that neutron bombardment of SiC results in the creation of silicon vacancies in the material. The lifetime of a positron associated with a boron cage anion, dodecahydrododecaborate in aqueous nitrate solution, was 277 ± 10 ps, compared with previous measurements of the cage compound in solid state which yielded 268 ± 8 ps. Competition for positrons between nitrate anion and the boron cage was measured.

15. SUBJECT TERMS

Positron, Positron Annihilation Lifetime Spectroscopy, PALS, voids in materials, positrons in tungsten, positrons in silicon carbide, positrons in neutron irradiated silicon carbide, positrons in aqueous solution, positrons in boron cage, electron scavenging

16. SECURITY CLASSIFICATION OF:			17. LIMITATION OF ABSTRACT	18. NUMBER OF PAGES	19a. NAME OF RESPONSIBLE PERSON
a. REPORT	b. ABSTRACT	c. THIS PAGE	UU	103	Dr. Larry W. Burggraf, AFIT/ENP
U	U	U			19b. TELEPHONE NUMBER *(Include area code)* (937) 255-3636 x4507, Larry.Burggraf@afit.edu